History of the sedimentary regimes of the Aquitaine margin (Bay of Biscay, France) at the outlet of its main tributaries during the last millennium: a mirror of the North Atlantic and European climates.

Eynaud, Frédérique [(1)], **Schmidt**, Sabine [(1)], **Iratcabal**, Vincent[(1,2)], **Dubosq**, Nicolas [(1)], **Billy** Isabelle[(1)], **Ther** Olivier[(1)] , **Deflandre**, Bruno [(1)]

[(1)] *Univ. Bordeaux, CNRS, Bordeaux INP, EPOC, UMR 5805, F-33600 Pessac, France*

[(2)] present address: *Geo-Ocean, Univ Bretagne Sud, Univ Brest, CNRS, Ifremer, UMR6538, F-56000 Vannes, France*

Corresponding author: Eynaud, Frédérique

<u>CrediT authorship contribution statement</u>

Eynaud, Frédérique: Writing – original draft, Methodology, Investigation, Visualization, Validation, Supervision, Project administration, Funding acquisition, Conceptualization.

Schmidt, Sabine: Writing – review & editing, Investigation, Formal analysis and interpretation of radionucleides.

Iratcabal, Vincent: review & editing.

Dubosq, Nicolas: review & editing.

Billy Isabelle: Methodology, Formal analysis, Data curation.

Ther Olivier: Methodology, Formal analysis, Data curation.

Deflandre, Bruno: Writing – review & editing, Project administration, Funding acquisition, Conceptualization of the JERICOBENT7 cruise.

<u>Keywords</u>

Last millennium, Northeastern Atlantic, Climate archives, Synoptic Hydrology, Hydrography, Bay of Biscay sediments

<u>Highlights</u>

River outlets in SW France are traps of past European hydroclimatic regimes
Bay of Biscay archives integrate the recent history of climatic and hydrological events
Neritic marine sediments reflect phenological records of the proximal continent
Marine archives of past centuries reveal local and global climate dynamics

<u>Research data</u>

All the core data referred to in the manuscript are available in the SEANOE (https://www.seanoe.org/) academic repository, at: https://doi.org/10.17882/104237

ABSTRACT

The location of two hemipelagic sequences, at the northern and southern edges of the Aquitaine shelf offers the possibility of obtaining a synoptic view of the southern Bay of Biscay oceanography, but also provides access to key contextual elements related to local and global forcing. These sequences were retrieved off the two main fluvial tributaries along the Aquitaine margin (southern Bay of Biscay) from the West Gironde mud patch and from the Capbreton canyon meanders. We focus on the interpretation of the sedimentological signal based on key X-ray fluorescence (XRF) elemental profiles along the cores for the last millennium. The robust and coherent new age models obtained for the two sequences allow us to tentatively relate the XRF signals to the hydroclimatological regime of the Bay of Biscay, and to compile and discuss a chronicle of the environmental changes at a regional scale, including the proximal continent, and in the larger synoptic view of the well-known European and North Atlantic historical frameworks. As expected, our results discriminate specific climatic trends, highlighting in particular the Medieval Warm Period, the Little Ice Age and the Current Warm Period. The climatic patterns identified during these specific phases are discussed in the light of recent advances in our knowledge of their modes of variability, and raise the question of teleconnections between the North Atlantic Oscillation, Atlantic sea-surface conditions and dynamics, together with atmospheric ones and especially storminess over Europe.

1. Introduction

Depositional centers along continental margins mark the outlet of numerous fluvial distributaries. These systems, nowadays connected inshore mostly by estuarine or lagoonal bays, reflect a geomorphological history shaped by sea-level changes during past glacial and interglacial climatic oscillations. Over at least the last million years, offshore depocenters have been alternately connected to and disconnected from their genetically related valleys in rhythms imposed by long-term orbital climatic shifts. Endmember sedimentary contexts can be considered according to these rhythms, with topographic huge incisions of epicontinental beds during sea-level lowstands (i.e., glacial maxima) contrasting with colmations of flooded valleys during highstands. In between those extreme states, falling or rising sea levels generate contrasted sedimentary gradients within the supply/ accommodation budgets along the main fluvial axes (e.g., Covault and Graham, 2010; Blum et al., 2013), thereby controlling the rates of sediment expulsion and deposit in the neritic zone.

Along modern continental shelves, past incised zones represent exceptional accumulation sites where the trapped sedimentological signals can be analysed at high temporal resolution to determine the evolution of hydrographic processes and the controlling factors at play. They also have the advantage of providing a coupled history of the oceanic and continental domains, and even of the adjacent coastlines (i.e., Sharman et al., 2021).

The continental margin of the Bay of Biscay, along the Atlantic border of the French metropolitan area, presents several depocenters, that form mud patches within the largest parts of the margin, all related to major fluvial routes, i.e., from North to South: the Loire ("Grande vasière"), Gironde/ Garonne ("West-Gironde mud patch") and Adour/Capbreton systems (Lesueur et al., 2001; Brocheray et al., 2014; Dubosq et al., 2021, 2022). These depocenters have already demonstrated their great interest in reconstructing past hydrological parameters of the mid-shelf of the Bay of Biscay during the Holocene and their exceptional sedimentation rates furthermore offer high-resolved records of the recent centuries (Mary et al., 2015, 2017; Mojtahid et al., 2018; Penaud et al., 2020). These archives document marine and terrestrial environmental changes, coupled or not, and provide access to key palaeoclimatic data such as: sea-surface temperature and salinity, past vegetation and rainfall regime over the catchment areas of the distributaries. This type of data is mostly reconstructed from micropaleontological tools. Their use in such archives can be challenging due to the dilution of fossil shells by fine mud particles, but the preserved corteges, on the other hand, record invaluable information in unprecedented temporal detail (i.e, annual), that are rarely reachable in the marine sediments. Such high-resolution signals are the key to defining climate trajectories beyond the instrumental period, and the targeted retrospective view also holds back from modern times, thus preventing misinterpretation of processes in overly anthropogenically biased systems.

Here we investigate and compare two sequences obtained from the Western Gironde Mud Pach (WGMP) and from the meanders of the Capbreton canyon (Figure 1). The modern sedimentary regimes dominating their location sites are directly influenced by the outflow of terrigeneous materials from the continent (e.g., volume of waters and of suspended sediment expulsed from the main tributaries), but also combine pelagic and benthic processes tied to the hydrology and hydrography of the Bay of Biscay (e.g., Lesueur et al., 2002; Mulder et al., 2011; Mary et al., 2015, 2017; Dubosq et al., 2021; Fontanier et al., 2023). The present work focuses on the comparison of some key XRF elemental profiles obtained along cores over the last millennium. The new robust and coherent age models obtained for the two sequences during the last centuries, allow us to tentatively relate the XRF signals to the hydroclimatological regime of the Bay of Biscay and of the proximal continent within the synoptic context of the well-known north Atlantic chronological and historical framework. We especially target the reconstruction of the hydroclimatic variability of the last 500 years, a period that encompasses the transition from the Little Ice Age (LIA) to the Common Warm Period (CWP, nomenclature after Björklund et al., 2023). At the scale of the northern hemisphere, the LIA appears as a relatively cold climatic pulse, accompanied by repeated and extensive advances of glaciers, with in the European Alps (see the synthesis of Nicolussi et al., 2022 on that topic), a phase of extension especially well documented from the 17th and 18th centuries of the Common Era (CE). Its duration, due to diachronic onsets depending on the area considered is not homogeneous but a consensus does exist on its termination (LIA from about 1400 to 1850 CE after Mangini et al. 2005; from 1250 to 1850 after Nicolussi et al. , 2022; from 1450-1850 Björklund et al., 2023). Coinciding also with the onset of the Industrial Era (IE), this recent climatic shift is of key importance to generate robust and comprehensive scenario of the processes governing current climatic changes and forecasts of their evolution.

2. Contextual elements regarding the studied sites

The position of the two studied sites, at the northern and southern edges of the Aquitaine shelf (Table 1, Figure 1), offers the possibility of gathering a synoptic view of the southern Bay of Biscay oceanography but also provides access to key contextual elements related to local parameters.

- Table 1 here -

Core label	*Cruise references, DOI*	*Latitude °N*	*Longitude ° E*	*Water depth (m)*	*Longitudinal distance (km) from the shore*	*References, Datasources*
MD03-2693	SEDICAR/PICABIA, SEDICAR MD 133, RV Marion Dufresne, BOURILLET Jean-François, TURON Jean-Louis (2003) https://doi.org/10.13155/36807	43.6543	-1.6634	431	15	**This work,** Gaudin et al., 2006, Mary et al., 2015
JB7-ST3c	JERICOBENT-7 cruise, RV Côtes De La Manche, DEFLANDRE Bruno (2019) https://doi.org/10.17600/18001022	45.6822	-1.6932	58	50	**This work**

Table 1: metadata of the studied sites

The first sequence, core MD03-2693, was retrieved in 2003 at 431 m from a terrace close to the Capbreton head and has already provided important achievements for the late Holocene paleoceanography (Gaudin et al., 2006; Brocheray et al., 2014; Mary et al., 2015, 2017). The second sequence, core JB7-ST3c, was retrieved in 2019 in the depocenter of the WGMP at 53 m water depth and constitutes a new and original record.

- Figure 1 here -

2.1 Summary of the structural, geological and sedimentary contexts

The two sites are located at the geomorphological edges of the Aquitanian shelf (Figure 1), limited to the south with the Basque country shelf by the Capbreton canyon and relayed to the North by the Armorican shelf (Bellec et al., 2009).

The structural and geological contexts of the Capbreton canyon have been extensively described in previous works conducted by the EPOC laboratory (e.g. from Boillot et al., 1973 to Bellec et al., 2009; and more recently Guiastrennec-Faugas et al., 2020). In summary, the canyon is the heritage of the complex tectonic history of the Bay of Biscay during the Mesozoic (opening) and Cenozoic (closure, concomitant with the Pyrenean orogen, e.g., Roca et al., 2011) and has, since then, been shaped by drastic changes (sea-level, climate, sedimentary fluxes, isostasy and biorhexistasy contexts) mainly related to glacio-eustatic controls during the Quaternary. The MD03-2693 coring site is located on a terrace overhanging the canyon axial thalweg by more than 100 m. No disturbance from gravity flows were evidenced in this sequence (Gaudin et al., 2006; Mary et al., 2015), despite turbiditic activity previously documented in the canyon (i.e., Mulder et al., 2001, 2012). Instead, this context seems to favor constant high sedimentation rates (~1 cm/yr) of fine-grained material (mean grain size of 15 µm, Mary et al., 2015) thought to be accumulated by processes related to sedimentation of nepheloid layers (Brocheray et al., 2014). Interestingly, the Capbreton canyon has been disconnected from the Adour river (its historical and natural main source of continental drainage) several times over the last millennium. In fact, the Adour estuary experienced natural migrations until the end of the 16th century (1578), when the mouth of the river was artificially fixed at Bayonne (Saint-Jours, 1921; Klingebiel and Legigan, 1978).

The Western Gironde Mud Patch (WGMP) is one of the largest depocenters marking the mid-shelf of the Bay of Biscay in front of French large drainage river systems. This peculiar, rather shallow environment, register since 600 years high sedimentation rates (~0.3 cm/yr, Lesueur et al., 2002) especially within the muddy depocenter from where core ST3C was retrieved. The WGMP has been genetically related to the Gironde outlet as evidenced by its bathymetric elongation and sedimentary signatures (Lesueur et al., 2001, 2002; Dubosq et al., 2021, 2022; Fontanier et al., 2022). Actually, the fine mud deposits, of 3 to 4 meters thick, lie on palimpsest levels rich in gravels and shells, covering a v-shaped unconformity structure oriented SW-NE and attributed to the incision(s) of a paleovalley in the Cenozoic substrate (probably the paleo-Gironde as suggested by the continuity with its modern northern pass, Lericolais et al., 1998; 2001; Lesueur et al., 2002).

2.2 Hydrographical contexts

At present, the study sites register sea-surface hydrographical conditions typical of the southern Bay of Biscay, thus related to a complex dynamical pattern marked by strong seasonal trends. The water masse structure and circulation over the mid-shelf are actually under the influence of dominant winds known to reverse within the year (e.g., Lazure et al., 2008; Charria et al., 2013; Solabarrieta et al., 2014). From spring to summer, weak winds and currents dominate and are preferentially directed from the north-west. The thermocline depth over the shelf varies between 20 and 50 m depth, and water stratification occurs in between May and October (Dubosq et al., 2022). On the opposite, from fall to winter, winds and currents change to a dominant southwesterly direction, with a deeper mixed layer reaching about 200 m under additional convection processes (Somavilla Cabrillo et al., 2011). A specific dynamic feature occur during some winters, with a warm surface poleward current running along the French coasts: this slope current is known as an extension of the Iberian Poleward Current and is called the Navidad Current (Garcia-Soto et al., 2002; Puillat et al., 2004; Lazure et al., 2008; Le Cann and Serpette, 2009; Charria et al., 2013; Solabarrieta et al., 2014). It roughly follows the poleward path of the European Slope Current (ESC), an important eastern boundary current that flows along the talus and is considered as a major component of the Atlantic Meridional Oceanic Circulation (AMOC). The latter also impacts the Bay of Biscay through the penetration of branches of the North Atlantic Current

(NAC), which enters the Bay from the North-West at 15°W of longitude (Figure 1, Pingree and Garcia-Soto, 2014; Xu et al., 2015; Martínez-García et al., 2023 ; Depuydt et al., 2024).

Just below the thermocline, the water column is occupied by the Eastern North Atlantic Waters (ENAW), showing relatively high temperature and salinity properties (VanAken et al., 2001). Circulations within the topmost meters of the water column are driven by a combination of factors such as tides, waves, winds and densities (Charria et al., 2013), and are thus highly variable in space and time. Fresh-water is supplied from several large tributaries (the Loire and Garonne French rivers being the largest ones, Puillat et al., 2004). They generate river plumes that can extend over the shelf but are reported to remain shoreward during the fall and winter seasons (Lazure and Jégou, 1998; Petus et al., 2010). As a result a winter hydrological front can occur, trapping suspended matter and low salinity waters in the inner part of the shelf (Lesueur et al, 2002). This front can be observed along the entire Armorican shelf and has important implication for the seasonal sedimentary regimes (Mojtahid et al., 2019; Penaud et al., 2020).

In the south-western part of the Bay of Biscay, the main freshwater distributary is the Adour river, which drains the Pyrenees together with the Nivelle river. The Adour is considered to be a relatively small river, with a water discharge at an annual average of 300 $m^3.s^{-1}$ (e.g. Petus et al., 2010), thus three orders of magnitude less that the total mean annual discharge from the Loire and Gironde rivers (for each, an annual freshwater outflow of about 900 $m^3.s^{-1}$ was estimated by Puillat et al. 2004 at the end of the 2Oth century). Any reader interested by recent monitoring and data updates can consult the website *http://www.hydro.eaufrance.fr.*

3. Methods

3.1 XRF element profiles

Profiles reflecting the along-core distribution of major and some minor elements were obtained from the non-destructive scan of bulk sediments (half-core sections) using the XRF-AVAATECH core-scanner facilities from the EPOC laboratory. This tool has proven its high potential in paleoceanography as a way to discriminate variations in the sedimentary sources and contexts especially in hemipelagic sequences (e.g., Richter et al., 2006; Rothwell, 2006; Groudace et al., 2019a and b).

For core MD03-2693, measurements were performed at a 2-cm interval. The signature of up to 24 elements were extracted, including Fe, Ca, Al, Sr, Br, Pb, and Ti, as discussed in Mary et al. (2015). Measurements for core JB7-ST3c were performed at a 1-cm interval and the signature of 14 elements was extracted. For this article, selected ratios were calculated identically along the two sequences and are presented here in order to highlight common /opposite features in the records.

3.2 Statistical treatments of XRF data

Two software programs were used to investigate the significance of XRF-detected element values based on the classical routine of multivariate ordination with principal component analysis (PCA) tests: PAST4.09 (Hammer et al., 2001, using the correlation matrix) and the newly developed software XELERATE v.3, specifically designed for XRF data treatment (Weltje et al., 2015). To further discriminate the distribution of elements along cores, and thanks to XELERATE options, a clustering was applied asking for the determination of 4 clusters (this clustering is based on the hierarchical cluster analysis of Wards which uses a minimum variance criterion, with determined clusters based on their Euclidian linking distance, and visualised by a dendrogram, e.g., XELERATE 3 software user guide manual).

As usually recommended, data were transformed in ratio to avoid misinterpretation of the values related to grainsize or water content changes along the core, or to the machine capacity (e.g. Weltje and Tjallingii, 2008; Croudace et al., 2019a). We have chosen to keep the same list of elements for the two cores, then to sum them and use this sum as the reference denominator. Data used for calculation and figures are thus not expressed as percentages but as ratio to this sum. The elements retained are: Al, Si, S, K, Ca, Ti, Mn, Fe, Br, Rb, Sr, Y, Zr, Pb.

3.3 Stratigraphical controls and age model construction

A total of 9 radiocarbon dates were obtained on the northern ST3c core thanks to the French national ARTEMIS facilities (Table 2). No additional dating was performed on core MD03-2693 and the age control points thus conform to the published ones in Mary et al. (2015), but with a revised calibration.

- Table 2 here -

Actually, similar methods were applied for the age calibration steps and construction of the age-depth modelling regressions of the studied records. Due to the continuous evolution of calibration curves (Heaton et al, 2020), raw radiocarbon ages (Table 2) were converted using Calib 8.1 but considering an adapted protocol justified by the fact that no adequate and robust local age reservoir values exist in the considered area. Modern existing data of the local age reservoir (i.e., from the online marine reservoir correction database of Reimer and Reimer, 2001, http://calib.org/marine/) concern only coastal systems and thus integrate anomalies from the margin boundary influences (including fluvial and phreatic sources) that lower the ^{14}C marine reservoir age. All raw ^{14}C ages were therefore calibrated and converted to calendar ages using the IntCal20 calibration curve (Reimer et al., 2020) with the recommended reservoir age correction of ~400 years. We have chosen to not apply the Marine20 calibration curve in order to circumscribe the problem of too young ages that can not be converted in calendar age using this new model. Radionuclide measurements (^{137}Cs and ^{210}Pb) complete the calibrated ages at the top of the studied cores (see Table 2 and Figure 2). These measurements confirm the appropriateness of the chosen age reservoir correction. The age models were thus built for each core combining ages derived from short-lived radionuclides and calibrated ^{14}C: the best fit was obtained with a linear interpolated regression for core MD03-2693 and with a degree 6 polynomial regression for core ST3c For this unpublished ST3c archive, Bayesian age distributions were tested using the *Undatable* software (Lougheed and Obrochta, 2019). The two age models obtained are compared on Figure 2.

- Figure2 here -

4. Results and discussion

The following sections discuss the results and interpretation of the XRF elemental signatures, including a core-to-core comparison of the data. Records worthy of recontextualisation on a larger synoptic scale are then confronted with (paleo)climatic series obtained from various types of archives or reconstructions, in order to identify key processes at play in the hydroclimatic dynamics of the last centuries.

4.1 Along core XRF elemental signatures: the common facts

Figure 3 presents the results of the two ordination analyses done using independent softwares (XELERATE and PAST4.09, see section 3.2) to facilitate an objective interpretation of the XRF data.

- Figure3 here -

Despite the slightly different calculation procedures inherent to the softwares, similar contrasting features are observed. These features are consistent along the studied cores (number of individuals n= 818 for core MD03-2693 and n= 320 for ST3c), even if calculation steps can generate reversed weights on the main PCA axis. For both cores (Fig. 3), these results discriminate **4 major poles** of elements when considering the PC1 and PC2 cross distributions:

- O**n the first PCA axis** (>50% of the variance after PAST and Xelerate for the two cores, Fig. 3.1 and 3.2), **one pole** is expressed with similar saturation weights **grouping Sr, Ca, S and Zr**. **At the opposite, a second pole** characterized by similar weights **for Fe, Ti, Br, Rb, Y, Pb** is observed.

- On **the second PCA axis** (>17% of the variance after PAST and Xelerate for the two cores, Fig. 3.1 and 3.2), close saturation weights are seen for the following elements: **Si, Al, K for one pole, contrasting** with high negative scores **for Br, Pb, Y and S for the other pole**.

Mn is the only element that records a distinct and incoherent signature between the two cores, probably reflecting different biogeochemical contexts for each site (either related to diagenetic processes, bottom water-masse qualities or to physiography, e.g. deeper bathymetry for core MD03-2693).

The mapping of the clustering done with XELERATE enables to transpose this ordination along the sedimentary record within the respective core sections covering the last millennium (Figures 3.1.c and 3.2.c, note the different color codes related to the clustering only). The oldest parts of the sediment records, both from the VOG and the from Capbreton terrace, are characterised by Ca, Sr and Zr dominant signatures, whereas the intermediate middle-part and the topmost deposits are rather marked by a signature mixing terrigenous elements (Ti, Fe, Rb especially).

Following the results highlighted by the multivariate ordinations, six key elemental ratios have been compiled to highlight the difference between terrigenous sourced fractions versus marine carbonated (autochthonous pelagic and benthic) ones. Those ratios, i.e.: (Ca+Sr)/Si, (Si+Al+K+Ti)/(Br+Pb+Y), Ca/Sr, (Sr+Ca)/ (Rb+Fe), Fe/Zr, Ti/Si will be retained for the following steps of interpretation and discussions. Figure 4 compares their evolution over the common period covered by the studied cores, i.e., the last 800 years. Information on the migration of the Adour outlet is also added to recontextualize the history of this tributary.

- Figure4 here -

Strikingly similar trends can be seen over time, when the two sets of data are compared on the basis of XRF, since the beginning of the 14th century up to 1700 years CE, thus during the postmedieval warm period (Figure 4). This similar evolution provides a strong argument for common sedimentary trajectories followed by the two systems. However, after 1700 CE the VOG and the Capbreton sedimentary signals are no longer following the same trends (Figure 4). This is especially obvious after 1850 CE when entering the historical period of strong anthropogenic managements on landscapes and especially on coastal and fluvial banks. This date also coincides with the onset of the Commun Warm Period (CWP), which is also assimilated to the IE (Industrial era), and marks the entrance within the Anthropocene (as defined by Crutzen et al., 2001). Despite this terminal phase of divergence that can be explained by human induced disturbances, observations provided by the sedimentary XRF signals, suggest that over the last millennium, the two systems have been driven by a master synoptic forcing, at least sufficiently significant at the regional scale to homogeneize the mud record trapped in the offshore receptacles of the Gironde and Adour tributaries. The offshore recent sediments of the VOG and the Capbreton Canyon Terrace, due to their proximity to major river systems, integrate and mix material advections from continental and marine processes. The mid-latitude position of the Aquitaine basin relates it climatologically to an oceanic temperate regime, at present dominated by rainfall mainly in autumn and winter. The Gironde and the Adour drainage networks are submitted similarly to this primary forcing despite local microclimates (Lot and Tarn rivers are located at the Mediterranean boundary influence; the Basque country is known for its specific mild and humid microclimate…) but the nature of their sedimentary sources is highly variable given the geological units on which they depend. The two mountainous systems bordering the basin, i.e. the Pyrenees to the south and the Massif Central to the east are different enough in age and rock nature to generate distinctive particulate pools. The multi-centennial period covered by our data underlines few discrepancies between sedimentary trends (as deduced from the XRF measurements) from the southern and central parts of the Bay of Biscay. Impacts of major anthropic changes (such as the fixation of the Adour river outlet) on the sedimentary background seem to be undetectable before the 18^{th} century (coevolution stops around 1725 years CE); signals then follow divergent and even opposite evolutions. The temporal coherence observed in the signature of the selected elemental ratios is indicative of integrative processes also operating at the southern Bay of Biscay scale. At this time scale, only few forcing factors can produce such integration, and the best candidates appear to be related to climate, the only overarching driver that can control fluvial discharges together with the proximal oceanic regimes of the Bay, currents and marine productivity.

As previously identified on the basis of ordination (mapping of the cores on Fig. 3.1c and 3.2c), the transition between the Medieval Warm Period (MWP) and the Little Ice Age (LIA) shows a progressive decrease in the contribution of the Ca and Sr within the sediments in favour of terrigenous (Si, Ti, Fe…) material (Figure 4). At a first glance, this could be explained by the progressive cooling which accompanies this transition and thus by a diminution of the carbonated material from marine primary production in the Bay. However, this can also be seen as the dilution of this carbonate pole by a predominant advection of detrital sediment to the sea in relation to the LIA climatic pejoration. This period is actually known as recording tempestuous winters, more frequent and more intense storms, flooding events, that have strongly impacted shore geomorphologies over western Europe (e.g., Sorrel et al., 2012; Tessier et al., 2019). These two explanations are not mutually exclusive and once again argue for the important role of climatic variables on the sedimentary regimes of the Bay of Biscay over the last millennium.

4.2 Signals and their comparison with other regional sequences: an interpretative step beyond factually descriptive sedimentary regimes.

Given that one of the main factors modulating the sedimentary content of the studied sequences is related to climate, we have screened the literature to find similar records over the last millennium, especially those that mention atmospheric processes in the forces to discriminate. Few high-time-resolved qualitative archives do exist and all are based on indirect proxies from different terrestrial sites. Despite this limitation, we have compiled a selection of series related to temperature or climatic indexes from different sites in the proximal western European (Figure 5). Our approach benefited considerably from the integration in this compilation of a "local" signal from the Basque country, obtained after the dendrochronological study by Bourquin-Mignot and Girardclos (2001) on beeches (*Fagus sylvatica* L) from the Iraty forest (Fig.5a). Other key series documenting the last five centuries were considered at a broader geographical scale, with: Burgundy Spring Temperature anomalies derived from grape harvest dates (i.e. GHD, Fig.5b and 5c, after Chuine et al., 2004; Labbé et al., 2019); Spring temperatures reconstructed in Paris (Fig.5d Labbé et al., 2019); Alps temperature anomalies from the Mangini et al. (2005) stalagmite reconstruction (Fig.5e); with also Mean seasonal NAO index reconstructions (Winter means shown on Fig.5f) according to Luterbacher et al. (2001).

- Figure 5 here -

From this compilation over five centuries, many features can be highlighted when looking in detail at the different decadal events recorded, but the secular trends, compared as a whole, confirm that the sedimentary signals trapped off the coast of Aquitaine (shown here on the basis of core MD03-2693 only, as it represents - as seen previously - a regional integration and is the longest record, dark-blue curves in Figure 5) closely match the climatic trends observed at both local and European scales. This is particularly striking when marine sedimentary signals are compared with phenologically derived records: commonly paced evolutions, furthermore in the same ranges of amplitude, are seen along the past centuries (but also confirmed by Pearson correlation test, see Table 3). This clearly testifies a climatic synoptic control on recent, naturally built archives, both on land and at sea.

The best candidate among the primary factors able to govern the Bay of Biscay sedimentary signatures at the outlet of major fluvial tributaries, together with plant physiologies in the nearby European mountainous zones, is obviously related to macroscale processes, and thus to atmospheric dynamics. These dynamics are quantifiable in parameters such as temperature changes and precipitation budgets. Interesting is thus the comparison with the NAO oscillation winter index, known to modulate modern European temperatures and precipitations along strong north-south gradients (e.g., Dickson, 1997; Jalón-Rojas and Castelle, 2021). This is done on Figure 5f where the plot of the biogenic pole as recorded in the southern Bay of Biscay cores (with the ratio Sr+Ca/Rb+Fe) documents a lower marine carbonaceous content, classically attributed to cooler SSTs or larger terrigenous inputs, in close correlation with the variability of NAO values during negative situations of this index. In contrast, when this index is positive a decorrelation does occur, but low biogenic contents persist. It is interesting to take this parallelism a step further in relation to what has already been described by Jalón-Rojas and Castelle (2021) on some major fluvial distributaries in Europe for post-1959 years. Despite descriptive statistical results imprinted by anthropogenic biases (at least since the end of the LIA, i.e. mid-19th century), their study demonstrated that, since some decades, European climatic indices of variability (such as NAO, and their variant called WEPA -West Europe Pressure Anomalies) are relevant to explain precipitation and river discharges, with positive values documenting higher river discharges in Europe north of 41°N and higher precipitations in winter. Their results can echo our observations backcasting five centuries on Figure 5, since the beginning of the 16th century, arguing for a robust atmospheric pattern in place in the Northern hemisphere whatever decadal climatic variabilities.

Compared to phenological proxies, these positive phases are coherent with slightly higher mean growth indices of beeches in SW France and with positive temperature anomalies as deduced from Grape Harvest Dates (GHD) in NE France. They are also consistent with positive temperature anomalies of up to 2 degrees in the Alps (Fig.5e) but not systematically over the whole period covered. The “warm pulses” are consistent with what is known about modern NAO-positive situations, with milder temperatures recorded in the northern latitudes of Europe (e.g, Dawson et al., 2004), something our compilation also robustly documents, but only after 1850. In fact, there are numerous other warm pulses registered back in time, but not all of them coincide with positive NAO modes. The same is true for the coldest events, as recorded after phenological data (green vertical bars on Figure 5): they are occurring during negative NAO dominant situations, but conversely, they do not show a peak-to-peak coherency with central Alps temperatures, and rather occur indifferently during coldest or warmest periods of anomalies in Eastern Europe. This implies either: (a) that the targeted reference archive, located in the Central Alps of Austria (Mangini et al., 2005), may be located at the eastern or high altitude (>2500 m) limbs of the NAO influence, or (b) that the NAO temperature gradient patterns may have changed over time. This question has been recently tackled by Song et al. (2024), considering the geographical migration of the NAO centers, and their eastward shift (20°) during the late 20th century (1981-2001), which have strongly influenced the distribution of temperature patterns over Europe, together with the North Atlantic SST gradients.

Interestingly, and arguing for the quality of the selected archives and their robustness with respect to paleoclimate significance, the Alps temperature anomalies correlated well to the Ti/Si ratio of our sediment cores (Pearson correlation coefficient of -0,53, Fig.5e, Table 3). This relationship emphasises that the decadal or infrasecular variability captured by the sediment regime oscillations on the Atlantic front is consistent with significant climate changes at the synoptic scale in Europe. This is also true when comparing the other compiled indices and is especially relevant before the CWP/IE (i.e. 1850 CE). Some observations are especially key to underline before this date and during the late LIA (1700-1850), and point to coherent evolutions: between Paris spring temperatures (published in Labbé et al., 2019) and the Fe/Zr ratio (Pearson correlation coefficient of 0.34, Fig.5d, Table 3) and between growth indices from the Iraty forest and the Ca/Sr (Figure 5).

As already stated before, the decades after 1850 show pronounced trends with a strong overprint of the global warming signal during the last decades of the 20th century. In fact, it is also worth noting that cumulative periods of positive NAO seem to occur since the beginning of the CWP/IE (Figure 5f, after Luterbacher et al., 2001), thus promoting warmer SST contexts in the Bay of Biscay (e.g. Dawson et al., 2004). This onset also corresponds to marked changes in the sedimentary signatures of the southern Bay of Biscay with for instance highest values of the Ca/Sr and Fe/Zr ratios (Figure 5). For this latter ratio, it is noteworthy that the ST3c record shows an opposite trend (Figure 4), further underlining that the Adour versus the Gironde offshore systems function in a decoupled way after 1850. Previous interpretation of Fe quantification with XRF techniques in marine cores of the Bay of Biscay have correlated it to siliciclastic inputs (e.g., Motjahid et al., 2019) while Zr is often used as a proxy for grain-size (e.g., Penaud et al., 2020) or even for changes of flow velocity (Toucanne et al., 2021). Fe is also among a major redox-sensitive elements (Croudace et al., 2019b). Thus, in recent sediment layers as those pointed out in this discussion, it may also integrate biases related to organic carbon budgets. Together with the Ca/Sr ratio, it may reflect large changes in the overall carbon budget (including inorganic) since a few decades.

All these findings converge on the fact that the 20th century is an outlier in marine sedimentary archives, as already seen in major upwelling centers (e.g., McGregor and Mulitza, 2007), in the Artic (e.g., Falardeau et al., 2023), and in the Labrador Sea (e.g., Thibodeau et al., 2010) among other key areas, and thus also in the ocean dynamics (e.g., Dickson et al., 2002; Levitus et al., 2005).

5. A climate chronicle over 1000 years: processes and feedbacks linking the North Atlantic basin, Europe and shores of the southern Bay of Biscay

Backcasting approaches are just as important as forecasting approaches in promoting a sound understanding of climate processes. Extending correlation exercises of climate indices further into the past is of great importance for progress in correctly identifying the feedbacks involved and correctly defining the initial states and triggers of the observed climatic trends over the last century, a period which is fortunately covered by instrumental data, but which is considerably biased by anthropogenic artefacts. The limitations of the approach lie in the uncertainties inherent in the interpretation of proxies archived in sediments, and in the qualitative value of such an indirect way of generating climate data and series, but more than 60 years of Paleosciences have provided access to robust methods (e.g., Li et al., 2010), as have past reconstructions. This has led to the construction of Figure 6, which brings together climate-related indices over the last millennium. In order to synthetize the main findings of our study, and to illustrate and further identify the processes at play, we have selected and compiled:

- the PAGES 2k Network consortium reconstructions of temperature anomalies in Europe (Fig6a,: Europe standardized values -SD- relative to: 1500-2003; regional reconstruction series from the Database S2 - 11 April 2013 version, data available at https://www.ncei.noaa.gov/access/paleo-search/study/14188), resulting from an international compilation effort (PAGES 2k Consortium, 2013),
- phenological data as already presented for the last 500 years (Fig6e,f), here with the idea of illustrating what is registered along a SW - NE axis from two poles in France; and the derived temperatures anomalies (Fig6d) in Burgundy,
- sea-surface parameters in core MD03-2693 (off Capbreton) in Summer (July-August-September mean, at zero m): temperatures and salinities (Fig6b) as reconstructed from foraminifera assemblages (see Mary et al., 2015, 2017; Eynaud et al., 2018, 2021, 2022 for data and methods),
- the Mean annual Bordeaux Rainfall (in mm) per decadal period during the 19th century (Fig6j) as published in Fabre et al. (1939),
- detrented XRF data from the two studied marine cores (Fig6c, h, i) giving access to the evolution of the biogenic carbonaceous fractions, classically considered as proxies of oceanic temperatures. Their plot as detrented series is useful to better discriminate climate variables; interestingly, it obliterates the decorrelation of the core signals since the CWP (as previously seen without detrenting).

- Figure 6 here -

The Figure 6 additionally shows the climatic events that have affected Aquitaine, as compiled by Saint-Jours (1921) from the historical literature, thus providing a rich chronicle of this region. Saint-Jours (1921), with a total ignorance on modes and feedbacks driving the climate variability (hypotheses were constructed before the validation of the astronomical forcing on climate and the ice-age theory), proposed conclusions for the geomorphological evolution of Aquitaine coastal environments, worth to re-evaluate in the perspective of our modern knowledges. In fact, even if most of his deductions regarding the geomorphological processes at play were incorrect, his work has collected valuable observations and data, especially relevant at the scale of our study, and then precious to integrate in the framework of this compilation.

Figure 6 allows us to unambiguously discriminate the climatic pejoration of the LIA (and especially its late part, i.e. Nicolussi et al.,2022) within the last millennium: warmest conditions are registered before, up to the 15th century, and after during the CWP. In the Bay of Biscay, it is supported by both reconstructed oceanic temperatures and sedimentological proxies, and is also consistent with the warm events referenced on land by Saint-Jours (1921). In the second chapter, devoted to the history of the formation of the dunes, the author mentions the year 1248 CE as the hottest year in the northern hemisphere, and points out the cultivation of grapes on coastal dunes ("sand wines") at the end of the medieval period until the 16th century, with harvests occurring early in the second part of August. His year-to-year compilation (Chapter 5) of "summers of intense heat" in Gascony matches the trends detected with the sedimentological signals (Figure 6), as it does also for the list of "rigorous winters", which occur mainly during the cold LIA phase, as detected off Capbreton. Indeed, within the MD03-2693 record, the LIA recorded summer sea-surface temperatures below their modern average of 18°C (Fig6b, see also Figure 3b of Mary et al., 2017). These cooling periods coincide with a reduction in the tree growth indices in the Iraty Forest (Fig6f), related to cold climatic pulses by Bourquin-Mignot and Girardclos (2001). They also coincide with low spring temperatures in Burgundy (Fig6e, below 15°C, Labbé et al., 2019) and dominant negative NAO situations (Winter means shown on Fig.5f after Luterbacher et al., 2001), and are therefore showing an evolution of the atmospheric variables that is consistent with the known scheme for the latitudinal band that is the target of our study (45°N ± 0.5°), i.e. coldest and potentially stormiest contexts.

During the LIA, storminess is not homogeneously distributed across Europe, but rather a contrasting pattern has been suggested by the recent literature, with southern latitudes being more affected by storms and northern latitudes being less affected (in contrast to what was recorded during the MWP, e.g., Sorrel et al., 2012; Orme et al., 2021, Hess et al., 2023). Recent works (e.g., Hess et al., 2023) have also suggested that this LIA situation may be accompanied by storms extending over several seasons during the year, rather than just during winter. This pattern relates to the storm tracks and their main directions, which are in turn driven by the North Atlantic SST, the NAO and the AMOC via the dynamics of the subpolar gyre (SPG), each of these variables being strongly correlated with the others in a way that is not easy to disentangle, either now or in the past (Rodwell et al., 1999; Dawson et al., 2004; Sorrel et al., 2012; Olsen et al., 2012; Goslin et al., 2018; Lapointe and Bradley, 2021). During the LIA specific interval, the cited literature converges to identify a NAO negative situation (consistent with data from Luterbacher et al., 2001) with a weakening of the SPG. As previously introduced, longitudinal migration of the NAO centers (southern centers especially) was observed during the last 60 years in connection with changes in the North Atlantic SST tripole dynamics (e.g., Song et al., 2024). This tripole is defined as a contrast between SST anomalies in the tropical and subpolar North Atlantic (positive tripole= cold / negative = warm in this area) and in the southeast of Newfoundland (positive= warm SST anomalies/ negative = cold in this latter area) and may then mirrors the SPG dynamics. Feedbacks between the NAO and the SST tripole are attested depending upon the seasons (Rodwell et al., 1999; Czaja and Frankignoul, 2002; Dawson et al., 2007; Song et al. 2024). Warm SST anomalies may thus act as a key driver in this dynamics and the question of the impact of oceanic heat waves naturally arises in this complex pattern.

Currently and in the past (e.g., Gimeno et al., 2014; Dacre et al., 2019; Skinner et al., 2023), intense poleward transport of moisture occurs throughout atmospheric rivers (ARs) generating heavy precipitations (rain, hail, snow) and floods over Europe. These rivers closely follow the North Atlantic drift corridor, illustrating a strong ocean-atmosphere coupling, with tropical SST anomalies (oceanic heat waves?) being the trigger for excess moisture in the troposphere. The coupling of ARs with NAO and SST has not been fully addressed, but the work of Lavers and Villarini (2013), based on the analysis of mean sea level pressure and vertically integrated horizontal water vapour transport, has brought important conclusions on the fact that a negative NAO pattern preferentially drives North Atlantic storm tracks and ARs over southern Europe (south of 45°N). This is consistent with the LIA situation observed in our compilation, and may explain the observed changes in the sedimentation regime of the Bay of Biscay by the largest terrigenous fluxes to the sea due to a southerly deviated storm track directly affecting this bay and its coasts. These authors also mention that the filamentary structure of the ARs is constrained by the low-level jet. The relationship of this process to the upper-level westerly jet is unclear, but interestingly, large-amplitude jet meanders are observed in the 21st century and are explained by rapid Arctic warming causing a weakening of the temperature gradients between low and high latitudes (Francis and Vavrus, 2015; Stendel et al., 2021). This question is worth addressing because wavy jets are currently generating peculiar meteorological situations, especially in summer, with the installation of unusually prolonged weather conditions (blocking, domes) of either cold or hot temperatures (expressed by cold spells as well as heat waves, storms and droughts, e.g. Francis and Vavrus, 2015), as recently experienced in France. According to Francis and Vavrus (2015), these situations of weaker poleward temperature gradients are indicative of a negative Arctic oscillation, "the umbrella" oscillation that drives and encompasses the regional NAO (e.g., Kerr, 1999). This implies that negative NAO phases occur in both hotter and colder climates, a conclusion that may reconcile some inconsistencies between modern and past observations of storminess in Europe during contrasting climatic episodes (see discussion in Section 4.2). Based on this observational assessment, it appears that the key to achieving robustness in the prediction of storminess in terms of track and intensity may lie in the identification of hydroclimatic processes linking atmospheric (tropospheric and stratospheric), oceanic and freshwater reservoirs (taking into account feedbacks from ice sheets in colder climates), with particular emphasis on the issue of seasonality.

Could the records from the Bay of Biscay help to support this? If we look at the recovered warmest phases, i.e., the MWP and the CWP, arguments can be identified considering the oceanographic regime detected in the Bay. Warm spells (summer SST above modern values and abundant calcareous biogenic contents) mostly align with saltier surface-waters (Fig6b). Currently, such configurations are associated with intrusions of the warm surface poleward Navidad Current, which follows the path of the ESC and preferentially advects warm and salty subtropical waters into the Bay in winter (Le Cann and Serpette, 2009). According to Garcia-Soto et al. (2002), winter warmings in the southern Bay of Biscay, associated with Navidad years, correlate with a low NAO index for the preceding November–December months (ending the fall season). The implication is that, once again, negative NAO situations are key shifting phases in the dynamics of regional currents on a seasonal scale. Interestingly, the Bordeaux rainfall data from the 19th century (Fabre et al., 1939, Fig6g) suggest that high salinity coincides with high precipitation: this is thus also in line with a negative NAO pattern and storm tracks and ARs preferentially directed towards southern Europe (south of 45°N). Based on a chronicle of 9 years of hydrographic data from the 1990s, and despite high inter-annual variability, Puillat et al. (2004) found that surface salinities higher than 35 occur from spring to late summer in the inner bay, with a cross-shore / along-shore distribution of isohalines explained by river discharges and the mean wind direction during the previous 6 months (SW from fall to the end of winter, NW from spring to the end of summer ; Puillat et al. 2004). All these observations in the bay are therefore puzzling and it is not easy to reconcile them in order to hypothesise a theoretical hydrographic model that can be applied whatever the time scales. This shows the need for a major effort to collect climatological, meteorological and hydrographic data (instrumental and reconstructed) over several centuries in order to make progress in understanding the processes governing the environmental evolution of the Aquitaine territories, both offshore and onshore. As this region is a crossroads in terms of latitude for better understanding the variability of storm tracks, such work could benefit the entire European coast.

6. Conclusion

The aim of the present work was twofold: firstly, to assess, on the basis of two marine archives with high sedimentation rates, their potential for capturing the hydroclimatic variability of the last millennium at the regional scale of the southern Bay of Biscay, including the proximal Aquitaine land territories (in an integrated picture from source to sink); and, secondly, from the compilation of these archives with comparable series, to construct and discuss a chronicle of events affecting this region over several centuries, during key periods of contrasting climatic situations (i.e., MWP, LIA and the CWP) also recognized at the synoptic scale of the North Atlantic region.

Our study suggests that a core-to-core comparative approach is needed to validate both the information trapped within the sedimentary signals and their age scaling (even in the frame of robust dating controls): the two series complement each-other and the focus on common features detected helps to avoid misinterpretation or erroneous attributions (bias due to local effects). This method thus provides a robust historical scenario for the evolution of the Bay of Biscay basin. A further step can certainly be taken in future studies with the generation of stacked records for this basin.

Our results show that the mid-latitude of 45°N in the Northeastern Atlantic is a strategic location to investigate hydroclimatic teleconnections. Its axial position with respect to the NAO pattern balance between southern and northern Europe, particularly with regard to storm tracks, is reflected in the sensitivity of the studied archives. The last 150 years are shown to be exceptional in the context of the last millennium with a trend consistently attributed to the CWP following the colder LIA, but also integrating impacts of managements carried out on lands, shores and rivers carried out at that time. The combination of undetrended/detrented series highlights this particular feature within the records. The end of the MWP occurs in the mid-15th century and is characterised in the Bay of Biscay by higher terrigenous contents and cooler SST due to a shift towards stormy conditions, consistent with the negative dominant NAO patterns during the LIA. During the last phase of the LIA, data from oceanic proxies reveal sub-centennial trends comparable to those identified with phenologically derived ones as seen in the nearby Basque forests and in Burgundy, but also consistent with temperature reconstructions from the Alps and Paris. It suggests the existence of an atmospheric corridor, i.e. a baroclinic structure (constrained by orogenic relief?), which persists along an axial direction around 45°N. In this perspective, the development of indices from specific continental locations north and south of this axis, and their testing along long-term chronicles, could complement our knowledge of the evolution of climatic variables. We are convinced that prediction tools cannot be developed in a valuable way without the effort of integrating long-term trends in the past. These reconstructions remain the only way to decipher natural processes and their teleconnections.

7. Declaration of competing interest

The authors declare that they have no competing financial interests or personal relationships that could have appeared to influence the work reported in this paper.

8. Data availability

All the core data referred to in the manuscript are available in the SEANOE (https://www.seanoe.org/) academic repository, at: https://doi.org/10.17882/104237

9. Acknowledgments

This work was supported by the ANR HAMOC Project ("Holocene North-Atlantic Gyres and Mediterranean Overturning Dynamic through Climate Changes" - Grant ANR-13-BS06-0003), and the national funding to the PPR-RiOMar project through the Agence Nationale de la Recherche for France 2030 under the reference ANR-22-POCE-0006. Fundings were also obtained for the analyses thanks to the CNRS French INSU actions: TelluS-ARTEMIS CONTINUHHUM-2022 and TelluS-ARTEMIS PaléoVOG-2021; TelluS-Action Post-Campagnes à la mer 2021, and the LEFE- EC2CO VOG project from the national program Interface LEFE-EC2CO. The JERICObent-7 cruise (10-15 July 2019 ; NR Côtes de la Manche) was funded by the French Oceanographic Fleet (DOI: 10.17600/18001022). We sincerely acknowledge the captain and the crew of the R/V "Côtes de la Manche" (CNRS-INSU) for their great help during the cruise.

10. References

Bellec, V.K., Cirac, P., Faugères, J.-C., 2009. Formation and evolution of paleo-valleys linked to a subsiding canyon, North Aquitaine shelf (France). Comptes Rendus Geoscience 341, 36–48. https://doi.org/10.1016/j.crte.2008.07.016

Björklund, J., Seftigen, K., Stoffel, M., Fonti, M.V., Kottlow, S., Frank, D.C., Esper, J., Fonti, P., Goosse, H., Grudd, H., Gunnarson, B.E., Nievergelt, D., Pellizzari, E., Carrer, M., Von Arx, G., 2023. Fennoscandian tree-ring anatomy shows a warmer modern than medieval climate. Nature 620, 97–103. https://doi.org/10.1038/s41586-023-06176-4

Blum, M., Martin, J., Milliken, K., Garvin, M., 2013. Paleovalley systems: Insights from Quaternary analogs and experiments. Earth-Science Reviews 116, 128–169. https://doi.org/10.1016/j.earscirev.2012.09.003

Boillot, G., Dupeuble, PA., Hennequin-Marchand, I., Lamboy, M., Leprêtre, J-P., 1973. Carte géologique du plateau continental nord-espagnol entre le canyon de Capbreton et le canyon d'Aviles. Bull Soc Géol Fr 7:367–391

Bourquin-Mignot, C., Girardclos, O., 2001. Construction d'une longue chronologie de hêtres au Pays-basque. La forêt d'Iraty et le Petit Âge Glaciaire. In: Sud-Ouest européen, tome 11-Environnement et anthropisation, pp. 59-71. https://doi.org/10.3406/rgpso.2001.2767

Brocheray, S., Cremer, M., Zaragosi, S., Schmidt, S., Eynaud, F., Rossignol, L., Gillet, H., 2014. 2000years of frequent turbidite activity in the Capbreton Canyon (Bay of Biscay). Marine Geology 347, 136–152. https://doi.org/10.1016/j.margeo.2013.11.009

Czaja, A., Frankignoul, C., 2002. Observed Impact of Atlantic SST Anomalies on the North Atlantic Oscillation. J. Climate 15, 606–623. https://doi.org/10.1175/1520-0442(2002)015<0606:OIOASA>2.0.CO;2

Charria, G., Lazure, P., Le Cann, B., Serpette, A., Reverdin, G., Louazel, S., Batifoulier, F., Dumas, F., Pichon, A., Morel, Y., 2013. Surface layer circulation derived from Lagrangian drifters in the Bay of Biscay. Journal of Marine Systems 109–110, S60–S76. https://doi.org/10.1016/j.jmarsys.2011.09.015

Chuine, I., Yiou, P., Viovy, N., Seguin, B., Daux, V., Ladurie, E.L.R., 2004. Grape ripening as a past climate indicator. Nature 432, 289–290. https://doi.org/10.1038/432289a

Croudace, I.W., Löwemark, L., Tjallingii, R., Zolitschka, B., 2019a. Current perspectives on the capabilities of high resolution XRF core scanners. Quaternary International 514, 5–15. https://doi.org/10.1016/j.quaint.2019.04.002

Croudace, I.W., Löwemark, L., Tjallingii, R., Zolitschka, B., 2019b. High resolution XRF core scanners: A key tool for the environmental and palaeoclimate sciences. Quaternary International 514, 1–4. https://doi.org/10.1016/j.quaint.2019.05.038

Dacre, H.F., Martínez-Alvarado, O., Mbengue, C.O., 2019. Linking Atmospheric Rivers and Warm Conveyor Belt Airflows. Journal of Hydrometeorology 20, 1183–1196. https://doi.org/10.1175/JHM-D-18-0175.1

Dawson, A., Elliott, L., Noone, S., Hickey, K., Holt, T., Wadhams, P., Foster, I., 2004. Historical storminess and climate 'see-saws' in the North Atlantic region. Marine Geology 210, 247–259. https://doi.org/10.1016/j.margeo.2004.05.011

Dickson, B., 1997. From the Labrador Sea to global change. Nature 386, 649–650. https://doi.org/10.1038/386649a0

Dickson, B., Yashayaev, I., Meincke, J., Turrell, B., Dye, S., Holfort, J., 2002. Rapid freshening of the deep North Atlantic Ocean over the past four decades. Nature 416, 832–837. https://doi.org/10.1038/416832a

Depuydt, P., Toucanne, S., Barras, C., Le Houedec, S., Mojtahid, M., 2024. Last Glacial – Holocene variability of the European Slope Current, NE Atlantic. Palaeogeography, Palaeoclimatology, Palaeoecology 633, 111884. https://doi.org/10.1016/j.palaeo.2023.111884

Dubosq, N., Schmidt, S., Sudre, J., Rigaud, S, Lamarque, B., Danilo, M., Grémare, A., Deflandre, B., 2022. First observations of seasonal bottom water deoxygenation off the Gironde estuary (Bay of Biscay, North East Atlantic). Front. Mar. Sci. 9:1006453. https://doi: 10.3389/fmars.2022.1006453

Dubosq, N., Schmidt, S., Walsh, J.P., Grémare, A., Gillet, H., Lebleu, P., Poirier, D., Perello, M.-C., Lamarque, B., Deflandre, B., 2021. A first assessment of organic carbon burial in the West Gironde Mud Patch (Bay of Biscay). Continental Shelf Research 221, 104419. https://doi.org/10.1016/j.csr.2021.104419

Eynaud, F., Mary, Y., Zumaque, J., Wary, M., Gasparotto, M.-C., Swingedouw, D., Colin, C., 2018. Compiling multiproxy quantitative hydrographic data from Holocene marine archives in the North

Atlantic: A way to decipher oceanic and climatic dynamics and natural modes? Global and Planetary Change 170, 48–61. https://doi.org/10.1016/j.gloplacha.2018.07.017

Eynaud, F., Verdin, F., Mary, Y., Beaudouin, C., López-Romero, E., Penaud, A., Colin, C., Culioli, C., 2022. Holocene climate dynamics on the European scale: Insights from a coastal archaeological record from the temperate Bay of Biscay (SW France). Quaternary International 613, 46–60. https://doi.org/10.1016/j.quaint.2021.09.018

Eynaud, F., Zaragosi, S., Wary, M., Woussen, E., Rossignol, L., Voisin, A., 2021. Are Past Sea-Ice Reconstructions Based on Planktonic Foraminifera Realistic? Study of the Last 50 ka as a Test to Validate Reconstructed Paleohydrography Derived from Transfer Functions Applied to Their Fossil Assemblages. Geosciences 11, 409. https://doi.org/10.3390/geosciences11100409

Fabre, L.A., 1905. Le sol de la Gascogne, in: La Géographie (Bulletin de La Société Géographique). Masson et Cie.

Falardeau, J., De Vernal, A., Seidenkrantz, M.-S., Fritz, M., Cronin, T.M., Gemery, L., Rochon, A., Carnero-Bravo, V., Hillaire-Marcel, C., Pearce, C., Archambault, P., 2023. A 1300-year microfaunal record from the Beaufort Sea shelf indicates exceptional climate-related environmental changes over the last two centuries. Palaeogeography, Palaeoclimatology, Palaeoecology 625, 111670. https://doi.org/10.1016/j.palaeo.2023.111670

Fontanier, C., Deflandre, B., Rigaud, S., Mamo, B., Dubosq, N., Lamarque, B., Langlet, D., Schmidt, S., Lebleu, P., Poirier, D., Cordier, M.A., Grémare, A., 2022. Live (stained) benthic foraminifera from the West-Gironde Mud Patch (Bay of Biscay, NE Atlantic): Assessing the reliability of bio-indicators in a complex shelf sedimentary unit. Continental Shelf Research 232, 104616. https://doi.org/10.1016/j.csr.2021.104616

Fontanier, C., Mamo, B., Dubosq, N., Lamarque, B., Rigaud, S., Schmidt, S., Lebleu, P., Poirier, D., Cordier, M.-A., Grémare, A., Deflandre, B., 2023. Seasonal variability of living benthic foraminifera from the West-Gironde mud patch (Bay of Biscay, NE Atlantic): Three contrasted periods under the stereomicroscope. Continental Shelf Research 268, 105117. https://doi.org/10.1016/j.csr.2023.105117

Francis, J.A., Vavrus, S.J., 2015. Evidence for a wavier jet stream in response to rapid Arctic warming. Environ. Res. Lett. 10, 014005. https://doi.org/10.1088/1748-9326/10/1/014005

Garcia-Soto, C., 2002. Navidad development in the southern Bay of Biscay: Climate change and swoddy structure from remote sensing and in situ measurements. Journal of Geophysical Research 107. https://doi.org/10.1029/2001JC001012

Gaudin, M., Mulder, T., Cirac, P., Berné, S., Imbert, P., 2006. Past and present sedimentary activity in the Capbreton Canyon, southern Bay of Biscay. Geo-Mar Lett 26, 331–345. https://doi.org/10.1007/s00367-006-0043-1

Gimeno, L., Nieto, R., VÃ¡zquez, M., Lavers, D.A., 2014. Atmospheric rivers: a mini-review. Front. Earth Sci. 2. https://doi.org/10.3389/feart.2014.00002

Goslin, J., Fruergaard, M., Sander, L., Gałka, M., Menviel, L., Monkenbusch, J., Thibault, N., Clemmensen, L.B., 2018. Holocene centennial to millennial shifts in North-Atlantic storminess and ocean dynamics. Sci Rep 8, 12778. https://doi.org/10.1038/s41598-018-29949-8

Guiastrennec-Faugas, L., Gillet, H., Silva Jacinto, R., Dennielou, B., Hanquiez, V., Schmidt, S., Simplet, L., Rousset, A., 2020. Upstream migrating knickpoints and related sedimentary processes in a submarine canyon from a rare 20-year morphobathymetric time-lapse (Capbreton submarine canyon, Bay of Biscay, France). Marine Geology 423, 106143. https://doi.org/10.1016/j.margeo.2020.106143

Hammer, Ø., Harper, D.A.T., and P. D. Ryan, 2001. PAST: Paleontological Statistics Software Package for Education and Data Analysis. Palaeontologia Electronica 4(1): 9pp.

Heaton, T.J., Köhler, P., Butzin, M., Bard, E., Reimer, R.W., Austin, W.E.N., Bronk Ramsey, C., Grootes, P.M., Hughen, K.A., Kromer, B., Reimer, P.J., Adkins, J., Burke, A., Cook, M.S., Olsen, J., Skinner, L.C., 2020. Marine20—The Marine Radiocarbon Age Calibration Curve (0–55,000 cal BP). Radiocarbon 62, 779–820. https://doi.org/10.1017/RDC.2020.68

Hess, K., Engel, M., Patel, T., Vakhrameeva, P., Koutsodendris, A., Klemt, E., Hansteen, T.H., Kempf, P., Dawson, S., Schön, I., Heyvaert, V.M.A., 2024. A 1500-year record of North Atlantic storm flooding from lacustrine sediments, Shetland Islands (UK). J Quaternary Science 39, 37–53. https://doi.org/10.1002/jqs.3568

Jalón-Rojas, I., Castelle, B., 2021. Climate Control of Multidecadal Variability in River Discharge and Precipitation in Western Europe. Water 13, 257. https://doi.org/10.3390/w13030257

Kerr, R.A., 1999. A New Force in High-Latitude Climate. Science 284, 241–242. DOI: 10.1126/science.284.5412.241

Klingebiel, A., Legigan, P., 1978. Histoire géologique des divagations de l'Adour. In: Proc Congr IVème Centenaire du Détournement de l'Adour 1578–1978. Bayonne Société des Sciences, Lettres et Arts de Bayonne, pp. 23–33.

Labbé, T., Pfister, C., Brönnimann, S., Rousseau, D., Franke, J., Bois, B., 2019. The longest homogeneous series of grape harvest dates, Beaune 1354-2018, and its significance for the understanding of past and present climate. Clim. Past, 15, 1485–1501, https://doi.org/10.5194/cp-15-1485-2019

Lapointe, F., Bradley, R.S., 2021. Little Ice Age abruptly triggered by intrusion of Atlantic waters into the Nordic Seas. Sci. Adv. 7, eabi8230. https://doi.org/10.1126/sciadv.abi8230

Lazure, P., Dumas, F., Vrignaud, C., 2008. Circulation on the Armorican shelf (Bay of Biscay) in autumn. Journal of Marine Systems 72, 218–237. https://doi.org/10.1016/j.jmarsys.2007.09.011

Lazure, P., Jegou, A.-M., 1998. 3D modelling of seasonal evolution of Loire and Gironde plumes on Biscay Bay continental shelf. Oceanologica Acta 21, 165–177. https://doi.org/10.1016/S0399-1784(98)80006-6

Le Cann, B., Serpette, A., 2009. Intense warm and saline upper ocean inflow in the southern Bay of Biscay in autumn–winter 2006–2007. Continental Shelf Research 29, 1014–1025. https://doi.org/10.1016/j.csr.2008.11.015

Levitus, S., Antonov, J., Boyer, T., 2005. Warming of the world ocean, 1955–2003. Geophysical Research Letters 32, 2004GL021592. https://doi.org/10.1029/2004GL021592

Lericolais, G., Fénies, H., Tastet, J.P., Berné, S., 1998. Reconnaissance par stratigraphie sismique haute résolution de la paléovallée de la Gironde sur le plateau continental - High resolution seismic stratigraphy of the Cironde paleovalley on the continental shelf. C. R. Acad. Sci. Paris, Sciences de la terre et des planetes / Earth & Planetary Sciences 326, 701 – 708.

Lericolais, G., Berné, S., Fénies, H., 2001. Seaward pinching out and internal stratigraphy of the Gironde incised valley on the shelf (vay of biscay). Marine Geology 175, 183–197.

Lesueur, P., Jouanneau, J.-M., Boust, D., Tastet, J.-P., Weber, O., 2001. Sedimentation rates and fluxes in the continental shelf mud fields in the Bay of Biscay (France). Continental Shelf Research 21, 1383–1401. https://doi.org/10.1016/S0278-4343(01)00004-8

Lesueur, P., Tastet, J.P., Weber, O., 2002. Origin and morphosedimentary evolution of fine-grained modern continental shelf deposits: the Gironde mud fields (Bay of Biscay, France). Sedimentology 49, 1299–1320. https://doi.org/10.1046/j.1365-3091.2002.00498.x

Li, B., Nychka, D.W., Ammann, C.M., 2010. The Value of Multiproxy Reconstruction of Past Climate. Journal of the American Statistical Association 105, 883–895. https://doi.org/10.1198/jasa.2010.ap09379

Lopez-Saez, J., Corona, C., Slamova, L., Huss, M., Daux, V., Nicolussi, K., Stoffel, M., 2024. Multiproxy tree ring reconstruction of glacier mass balance: insights from Pinus cembra trees growing near Silvretta Glacier (Swiss Alps). Clim. Past 20, 1251–1267. https://doi.org/10.5194/cp-20-1251-2024

Lougheed, B.C., Obrochta, S.P., 2019. A rapid, deterministic age-depth modeling routine for geological sequences with inherent depth uncertainty. Paleoceanogr. Paleoclimatol. 34, 122–133. https://doi.org/10.1029/2018PA003457

Luterbacher, J., Xoplaki, E., Dietrich, D., Jones, P.D., Davies, T.D., Portis, D., Gonzalez-Rouco, J.F., Von Storch, H., Gyalistras, D., Casty, C., Wanner, H., 2001. Extending North Atlantic oscillation reconstructions back to 1500. Atmospheric Science Letters 2, 114–124. https://doi.org/10.1006/asle.2002.0047

Nicolussi, K., Le Roy, M., Schlüchter, C., Stoffel, M., Wacker, L., 2022. The glacier advance at the onset of the Little Ice Age in the Alps: New evidence from Mont Miné and Morteratsch glaciers. The Holocene 32, 624–638. https://doi.org/10.1177/09596836221088247

Mangini, A., Spötl, C., Verdes, P., 2005. Reconstruction of temperature in the Central Alps during the past 2000 yr from a δ18O stalagmite record. Earth and Planetary Science Letters 235, 741–751. https://doi.org/10.1016/j.epsl.2005.05.010

Martínez-García, B., Pascual, A., Rodríguez-Lázaro, J., Bodego, A., 2023. Distribution of recent planktonic foraminifera in surface sediments of the Basque shelf (S Bay of Biscay): Oceanographic implications. Continental Shelf Research 263, 105011. https://doi.org/10.1016/j.csr.2023.105011

Mary, Y., Eynaud, F., Zaragosi, S., Malaizé, B., Cremer, M., Schmidt, S., 2015. High frequency environmental changes and deposition processes in a 2 kyr-long sedimentological record from the Cap-Breton canyon (Bay of Biscay). The Holocene 25, 348–365.

Mary, Y., Eynaud, F., Colin, C., Rossignol, L., Brocheray, S., Mojtahid, M., Garcia, J., Peral, M., Howa, H., Zaragosi, S., Cremer, M., 2017. Changes in Holocene meridional circulation and poleward Atlantic flow: the Bay of Biscay as a nodal point. Climate of the Past 13, 201–216. https://doi.org/10.5194/cp-13-201-2017

McGregor, H., Mulitza, S., 2007. Rapid 20th-century increase in coastal upwelling off northwest Africa revealed by high-resolution marine sediment cores. PAGES news 15, 28–30. https://doi.org/10.22498/pages.15.2.28

Mojtahid, M., Durand, M., Coste, P.-O., Toucanne, S., Howa, H., Nizou, J., Eynaud, F., Penaud, A., 2019. Millennial-scale Holocene hydrological changes in the northeast Atlantic: New insights from ‘ *La Grande Vasière* ’ mid-shelf mud belt. The Holocene 29, 467–480. https://doi.org/10.1177/0959683618816478

Olsen, J., Anderson, N.J., Knudsen, M.F., 2012. Variability of the North Atlantic Oscillation over the past 5,200 years. Nature Geosci 5, 808–812. https://doi.org/10.1038/ngeo1589

Orme, L.C., Reinhardt, L., Jones, R.T., Charman, D.J., Barkwith, A., Ellis, M.A., 2016. Aeolian sediment reconstructions from the Scottish Outer Hebrides: Late Holocene storminess and the role of the North Atlantic Oscillation. Quaternary Science Reviews 132, 15–25. https://doi.org/10.1016/j.quascirev.2015.10.045

PAGES 2k Consortium, 2013. Continental-scale temperature variability during the past two millennia. Nature Geoscience 6, 339–346. https://doi.org/10.1038/ngeo1797

Penaud, A., Ganne, A., Eynaud, F., Lambert, C., Coste, P.O., Herlédan, M., Vidal, M., Goslin, J., Stéphan, P., Charria, G., Pailler, Y., Durand, M., Zumaque, J., Mojtahid, M., 2020. Oceanic versus continental influences over the last 7 kyrs from a mid-shelf record in the northern Bay of Biscay (NE Atlantic). Quaternary Science Reviews 229, 106135. https://doi.org/10.1016/j.quascirev.2019.106135

Petus, C., Chust, G., Gohin, F., Doxaran, D., Froidefond, J.-M., Sagarminaga, Y., 2010. Estimating turbidity and total suspended matter in the Adour River plume (South Bay of Biscay) using MODIS 250-m imagery. Continental Shelf Research 30, 379–392. https://doi.org/10.1016/j.csr.2009.12.007

Pingree, R.D., Garcia-Soto, C., 2014. Plankton blooms, ocean circulation and the European slope current: Response to weather and climate in the Bay of Biscay and W English Channel (NE Atlantic). Deep Sea Research Part II: Topical Studies in Oceanography 106, 5–22. https://doi.org/10.1016/j.dsr2.2014.07.008

Puillat, I., Lazure, P., Jégou, A.M., Lampert, L., Miller, P.I., 2004. Hydrographical variability on the French continental shelf in the Bay of Biscay, during the 1990s. Continental Shelf Research 24, 1143–1163. https://doi.org/10.1016/j.csr.2004.02.008

Reimer PJ, Reimer RW, 2001. A marine reservoir correction database and on-line interface. Radiocarbon 43:461-3. see http://calib.org/marine/

Reimer, R.W., Richards, D.A., Scott, E.M., Southon, J.R., Turney, C.S.M., Wacker, L., Adolphi, F., Büntgen, U., Capano, M., Fahrni, S.M., Fogtmann-Schulz, A., Friedrich, R., Köhler, P., Kudsk, S., Miyake, F., Olsen, J., Reinig, F., Sakamoto, M., Sookdeo, A., Talamo, S., 2020. The IntCal20 Northern Hemisphere Radiocarbon Age Calibration Curve (0–55 cal kBP). Radiocarbon 62, 725–757. https://doi.org/10.1017/RDC.2020.41

Richter, T.O., Van Der Gaast, S., Koster, B., Vaars, A., Gieles, R., de Stigter, H.C., de Haas, H., Van Weering, T.C.E., 2006. The Avaatech XRF Core Scanner: technical description and applications to NE Atlantic sediments., in: Rothwell, R.G. (Ed.), New Techniques in Sediment Core Analysis. Geological Society Special Publications, London, pp. 39–50.

Roca, E., Muñoz, J.A., Ferrer, O., Ellouz, N., 2011. The role of the Bay of Biscay Mesozoic extensional structure in the configuration of the Pyrenean orogen: Constraints from the MARCONI deep seismic reflection survey. Tectonics 30, 2010TC002735. https://doi.org/10.1029/2010TC002735

Rodwell, M.J., Rowell, D.P., Folland, C.K., 1999. Oceanic forcing of the wintertime North Atlantic Oscillation and European climate. Nature 398, 320–323. https://doi.org/10.1038/18648

Rothwell, R.G., Rack, F.R., 2006. New techniques in sediment core analysis: an introduction. SP 267, 1–29. https://doi.org/10.1144/GSL.SP.2006.267.01.01 in Rothwell, R.G. (Ed.), 2006. New techniques in sediment core analysis. Geol. Soc. Lond Spec. Pub. 267.

Saint-Jours, B., 1921. Le littoral Gascon, Bordeaux. Marcel Mounastre-Pioamilh Libraire-Éditeur

Sharman, G.R., Covault, J.A., Stockli, D.F., Sickmann, Z.T., Malkowski, M.A., Johnstone, S.A., 2021. Detrital signals of coastal erosion and fluvial sediment supply during glacio-eustatic sea-level rise, Southern California, USA. Geology 49, 1501–1505. https://doi.org/10.1130/G49430.1

Skinner, C.B., Lora, J.M., Tabor, C., Zhu, J., 2023. Atmospheric River Contributions to Ice Sheet Hydroclimate at the Last Glacial Maximum. Geophysical Research Letters 50, e2022GL101750. https://doi.org/10.1029/2022GL101750

Song, X., Yin, Z., & Wang, H., 2024. Interdecadal changes in the links between late-winter NAO and North Atlantic tripole SST and possible mechanism. Geophysical Research Letters, 51, e2024GL110138. https://doi.org/10.1029/2024GL110138

Sorrel, P., Debret, M., Billeaud, I., Jaccard, S.L., McManus, J.F., Tessier, B., 2012. Persistent non-solar forcing of Holocene storm dynamics in coastal sedimentary archives. Nature Geoscience 5, 892–896. https://doi.org/10.1038/ngeo1619

Stendel, M., Francis, J., White, R., Williams, P.D., Woollings, T., 2021. The jet stream and climate change, in: Climate Change. Elsevier, pp. 327–357. https://doi.org/10.1016/B978-0-12-821575-3.00015-3

Sylvester, Z., Durkin, P., Covault, J.A., 2019. High curvatures drive river meandering. Geology 47, 263–266. https://doi.org/10.1130/G45608.1

Tessier, B., Poirier, C., Weill, P., Dezileau, L., Rieux, A., Mouazé, D., Fournier, J., Bonnot-Courtois, C., 2019. Evolution of a shelly beach ridge system over the last decades in a hypertidal open-coast embayment (western Mont-Saint-Michel Bay, NW France). In: Castelle, B. and Chaumillon, E. (eds.), Coastal Evolution under Climate Change along the Tropical Overseas and Temperate Metropolitan France. Journal of Coastal Research, Special Issue 88, 77–88. https://doi.org/10.2112/SI88-007.1

Thibodeau, B., De Vernal, A., Hillaire-Marcel, C., Mucci, A., 2010. Twentieth century warming in deep waters of the Gulf of St. Lawrence: A unique feature of the last millennium. Geophysical Research Letters 37, 2010GL044771. https://doi.org/10.1029/2010GL044771

Toucanne, S., Soulet, G., Vázquez Riveiros, N., Boswell, S.M., Dennielou, B., Waelbroeck, C., Bayon, G., Mojtahid, M., Bosq, M., Sabine, M., Zaragosi, S., Bourillet, J., Mercier, H., 2021. The North Atlantic Glacial Eastern Boundary Current as a Key Driver for Ice-Sheet—AMOC Interactions and Climate Instability. Paleoceanog and Paleoclimatol 36, e2020PA004068. https://doi.org/10.1029/2020PA004068

Van Aken, H.M., 2001. The hydrography of the mid-latitude Northeast Atlantic Ocean — Part III: the subducted thermocline water mass. Deep Sea Research Part I: Oceanographic Research Papers 48, 237–267. https://doi.org/10.1016/S0967-0637(00)00059-5

Weltje, G.J., Tjallingii, R., 2008. Calibration of XRF core scanners for quantitative geochemical logging of sediment cores: Theory and application. Earth and Planetary Science Letters 274, 423–438. https://doi.org/10.1016/j.epsl.2008.07.054

Weltje, G.J., Bloemsma, M.R., Tjallingii, R., Heslop, D., Röhl, U., Croudace, I.W., 2015. Prediction of Geochemical Composition from XRF Core Scanner Data: A New Multivariate Approach Including Automatic Selection of Calibration Samples and Quantification of Uncertainties. In: Croudace, I.W., Rothwell, R.G. (Eds.), Micro-XRF Studies of Sediment Cores, Developments in Palaeoenvironmental Research. Springer, Berlin Heidelberg, pp. 507–534. https://doi.org/10.1007/978-94-017-9849-5

Xu, W., Miller, P.I., Quartly, G.D., Pingree, R.D., 2015. Seasonality and interannual variability of the European Slope Current from 20years of altimeter data compared with in situ measurements. Remote Sensing of Environment 162, 196–207. https://doi.org/10.1016/j.rse.2015.02.008

Captions, figures and tables for “History of the sedimentary regimes of the Aquitaine margin (Bay of Biscay, France) at the outlet of its main tributaries during the last millennium: a mirror of the North Atlantic and European climates.”

Figure caption

Figure 1: maps of the studied sites with a focus on the Bay of Biscay margin. The regional scheme of the main surface currents is drawn after the compilation of modern hydrological surveys from Pingree and Garcia-Soto (2014): North Atlantic Current (NAC) in red, Iberian Poleward Current (IPC) and European Slope Current (ESC) in orange. The bathymetric shading is obtained after EMODNET (https://emodnet.ec.europa.eu/en). The topmost synoptic map mix bathymetric and modern SST information (blue to red: 0 to 25°c). The modern drainage network of the Aquitaine basin is schematized after mixing maps from the theoretical hydrographical network (RHT; Pela et al., 2012), showing only the main distributaries, together with the map published by Schaefer and Blanc (2002). For a complete detailed view of suborder networks, the reader is invited to visit the website https://www.reddit.com/r/france/comments/14r3ptm/cours_deau_de_france_en_fonction_par_leur_grand/?onetap_auto=true&one_tap=true#lightbox. Other sequences of interest (cited in the text) are also plotted. (For interpretation of the references to color in this figure legend, the reader is referred to the Web version of this article)

Figure 2: age-depth relationships for the two studied cores: MD03-2693 (blue) and ST3c (dark red). Marks locate the dated samples along depth and time thanks to radiocarbon and radionuclide analyses (see methods). Radiocarbon dates are corrected and calibrated thanks to the CALIB8.1.0. software (the plotted age values are obtained from the mean of the 1 sigma range, see Table 2). The two age models are shown on similar scales for comparison on the left, but the ST3c polynomial regression is enlarged along depth on the right panel to provide a better view of the obtained regression. Conventional temporal delimitations of climatic period, are indicated along the age axis after Björklund et al. (2023), with: the Roman warn period (RWP), the Medieval Warm Period (MWP; 950-1250 CE) also known as the Medieval Climate Anomaly, the Little Ice Age (LIA, 1450–1850 CE) and the Current Warm Period. For ST3c, the 1σ envelopes obtained with the *Undatable* software (Lougheed and Obrochta, 2019) are also shown (dotted lines) to validate the polynomial construction of the age model. (For interpretation of the references to color in this figure legend, the reader is referred to the Web version of this article)

Figure 3: results of ordination calculations thanks to the different protocols explained in the methodology section. Those ordinations are done in order to highlight major element signatures and to provide a pre-interpretation of their distribution along cores. Panels are separated vertically for each studied core (topmost 3.1 panel for MD03-2693 data and lower 3.2 panel for ST3c ones) but the same presentation is respected from the left to the right in order to highlight similarities in the

grouping of the XRF data. Note that color code for clustering with Xelerate (b and c columns, just refers to cluster order and thus differs in between cores). (For interpretation of the references to color in this figure legend, the reader is referred to the Web version of this article)

Figure 4: Comparison of the last millennial evolution of some key elemental ratios (determined after ordinations, see previous Figure 3), i.e.: (Ca+Sr)/Si, (Si+Al+K+Ti)/(Br+Pb+Y), Ca/Sr, (Sr+Ca)/ (Rb+Fe), Fe/Zr, Ti/Si, for the studied cores. The topmost timeline identifies the migration of the Adour outlet over the studied period and significant shifts have been reported with vertical pink bands. Since 1578, this outlet is artificially fixed at Bayonne (~20 km south of the Capbreton canyon). The large grey band identifies the Litlle Ice Age –LIA temporal range in its maximal duration (its onset is not consensually defined but is reported as occurring as soon as the mid-13th century in some references, e.g. Nicolussi et al., 2022). (For interpretation of the references to color in this figure legend, the reader is referred to the Web version of this article)

Figure 5: comparison of local and European climatic indexes with key XRF elemental ratio in core MD03-2693 along the last 5 centuries. The dendrochronological reconstruction (a) of Bourquin-Mignot et al. (2001) obtained on the Basque country beeches (*Fagus sylvatica* L) from the Iraty forest (redrawn from their Fig.5) offers a close geographical reference. Their mean growth indices (averaged on 20 years) is highlighted in green and is reproduced on some XRF graphs to highlight similar/opposite evolution trends. It is complemented by the plot of Burgundy Summer Temperature reconstructions derived from grape harvest dates with (b): April - August temp. anomalies v. 1960- 1989 reference period for Dijon, after Chuine et al., 2004, *data available at: https://www.euroclimhist.unibe.ch/en/*) and the revised series of Labbé et al., 2019 of April - July temperatures in (c) Dijon and (d) Paris (*online data at: https://cp.copernicus.org/articles/15/1485/2019/*). Larger scale European signals are here documented by the Mangini et al. (2005) reconstruction of temperature anomalies (e) derived from the SPA 12 stalagmite record retrieved in the Central Alps of Austria (*data available at:* https://catalog.data.gov/dataset/noaa-wds-paleoclimatology-mangini-et-al-2005-spannagel-cave-stalagmite-oxygen-isotope-data-and-2), and by the (f) Mean seasonal NAO index reconstructions (Winter values shown, with positive values in red and negative ones in blue) after Luterbacher et al. (2001, *data available at:* https://crudata.uea.ac.uk/cru/data/paleo/?_ga=2.126245582.2132006485.1701786496-1957487287.1701786495). Some datasets have been plotted with a smoothed filter calculated on 5 or 15 points thanks to the PAST4.09 software (Hammer et al., 2001, using the *Simple smoother* tool in the

Time series menu). The pale green vertical bars circumscribe cold periods after Bourquin-Mignot et al. (2001) whereas the yellow ones delimitate phases of positive NAO index in winter after Luterbacher et al. (2001). Note that since 1578 (black star on the bottom age scale), the Adour outlet is artificially fixed at Bayonne. (For interpretation of the references to color in this figure legend, the reader is referred to the Web version of this article)

Figure 6: selected climate related indices over the last milllenium. Phenological reconstructions (d, e, f) are reproduced from Figure 5. Core data related to the biogenic pole (c, h, i) are here compared to the PAGES 2k Network consortium reconstructions of temperature anomalies (a, *data available at https://www.ncei.noaa.gov/access/paleo-search/study/14188*). To highlight specific temporal features, a detrending of XRF data from the studied cores has been done with the PAST4.09 software (Hammer et al., 2001, with the *Remove trend* tool in the *Transform* menu, linear regression soustraction back to 693 BC for core MD03-2693). Thanks to the same software, smoothed filters have been applied on some series (15 points filter using the *Simple smoother* tool in the *Time series* menu). Despite their low resolution, Summer sea-surface (at zero m) temperatures and salinities (b) reconstructed after foraminifera assemblages in core MD03-2693 off Capbreton (see Mary et al., 2015, 2017; Eynaud et al., 2018, 2021, 2022 for data and methods) have been added, together with the Bordeaux Mean annual Rainfall (g, in mm) per decadal period during the 19th century as published in Fabre et al. (1939). The pale green vertical bars circumscribe cold periods (after Bourquin-Mignot et al. 2001, as done on Figure5), and climatic events have been reported after the historical literature compilation from Saint-Jours (1921). (For interpretation of the references to color in this figure legend, the reader is referred to the Web version of this article)

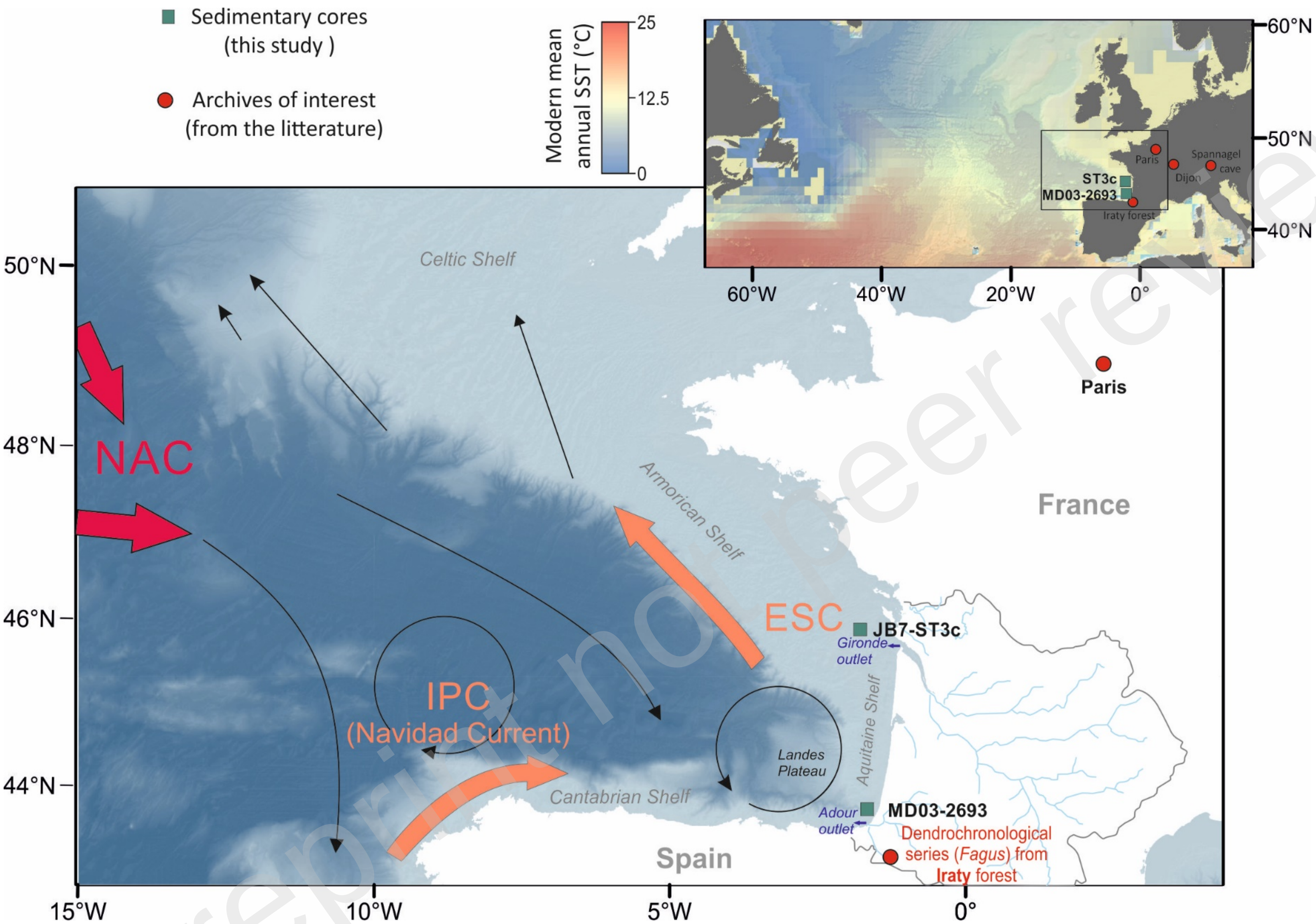
Sedimentary cores
(this study)
Archives of interest
(from the litterature)
Modern mean
annual SST (°C)
25
12.5
0
60°N
50°N
40°N
60°W
40°W
20°W
0°
Paris
Dijon
Spannagel
cave
ST3c
MD03-2693
Iraty forest
Celtic Shelf
50°N
48°N
46°N
44°N
NAC
Armorican Shelf
France
Paris
ESC
JB7-ST3c
Gironde
outlet
IPC
(Navidad Current)
Aquitaine Shelf
Landes
Plateau
Cantabrian Shelf
Adour
outlet
MD03-2693
Dendrochronological
series (Fagus) from
Iraty forest
Spain
15°W
10°W
5°W
0°

Figure 1

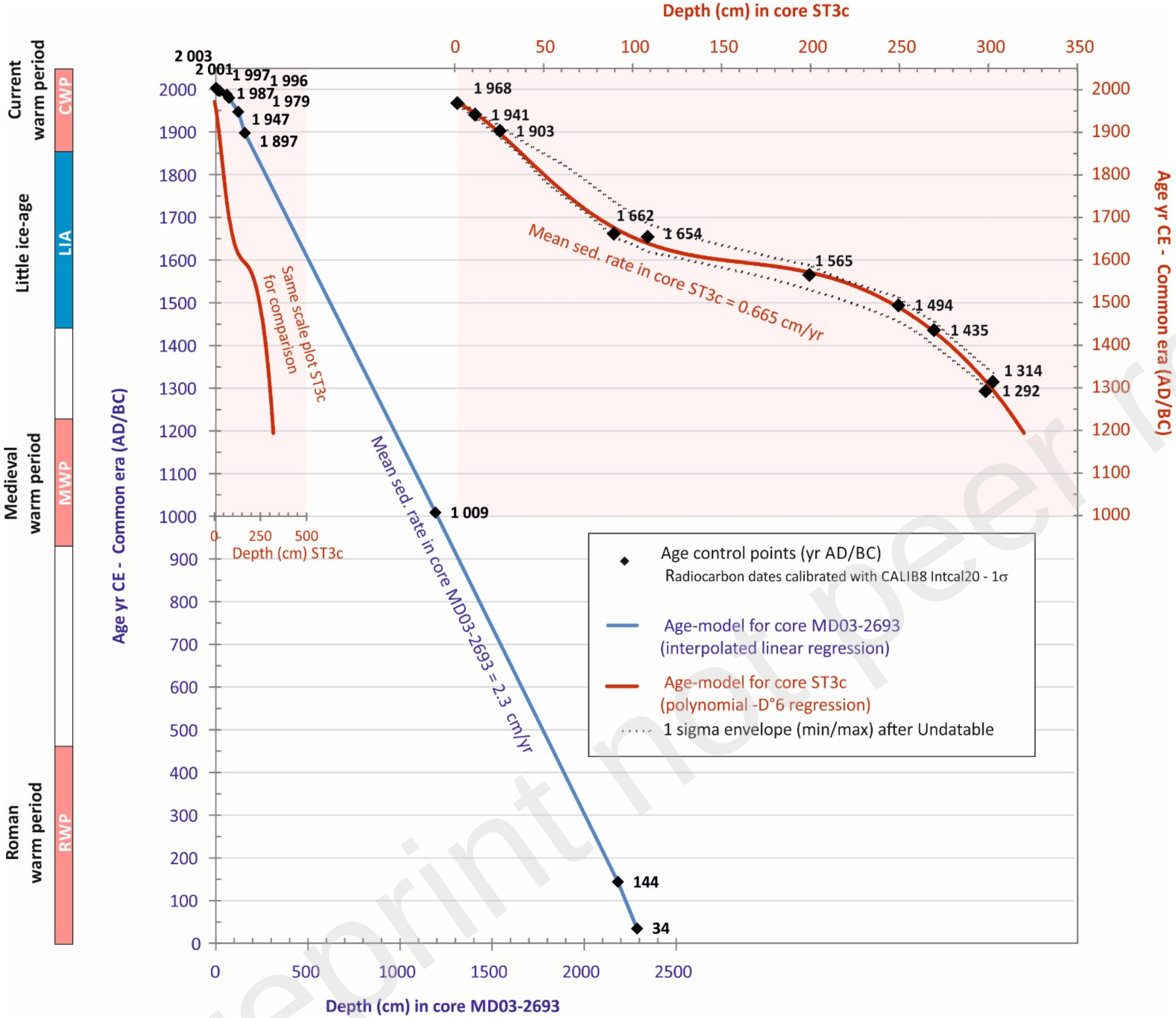
Depth (cm) in core ST3c
0
50
100
150
200
250
300
350
Current warm period
CWP
Little ice-age
LIA
Medieval warm period
MWP
Roman warm period
RWP
Age yr CE - Common era (AD/BC)
2 003
2 001
1 997
1 996
1 987
1 979
1 947
1 897
1 968
1 941
1 903
1 662
1 654
1 565
1 494
1 435
1 314
1 292
1 009
144
34
Same scale plot ST3c for comparison
Depth (cm) ST3c
Mean sed. rate in core ST3c = 0.665 cm/yr
Mean sed. rate in core MD03-2693 = 2.3 cm/yr
Age control points (yr AD/BC)
Radiocarbon dates calibrated with CALIB8 Intcal20 - 1σ
Age-model for core MD03-2693 (interpolated linear regression)
Age-model for core ST3c (polynomial -D°6 regression)
1 sigma envelope (min/max) after Undatable
Age yr CE - Common era (AD/BC)
Depth (cm) in core MD03-2693

Figure 2

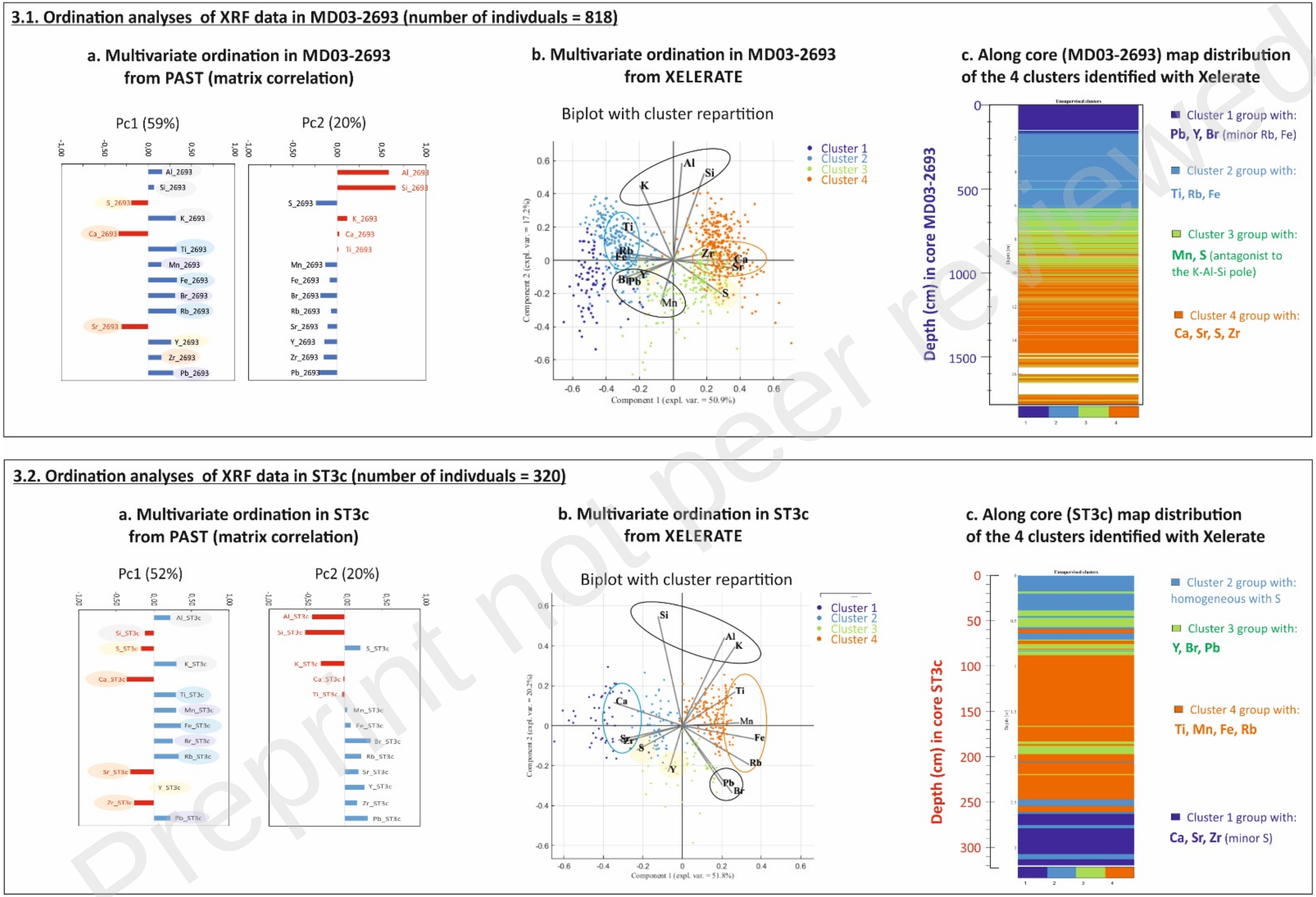
3.1. Ordination analyses of XRF data in MD03-2693 (number of indivduals = 818)
a. Multivariate ordination in MD03-2693 from PAST (matrix correlation)
Pc1 (59%)
Pc2 (20%)
b. Multivariate ordination in MD03-2693 from XELERATE
Biplot with cluster repartition
Cluster 1
Cluster 2
Cluster 3
Cluster 4
Component 1 (expl. var. = 50.9%)
Component 2 (expl. var. = 17.2%)
c. Along core (MD03-2693) map distribution of the 4 clusters identified with Xelerate
Depth (cm) in core MD03-2693
Cluster 1 group with: Pb, Y, Br (minor Rb, Fe)
Cluster 2 group with: Ti, Rb, Fe
Cluster 3 group with: Mn, S (antagonist to the K-Al-Si pole)
Cluster 4 group with: Ca, Sr, S, Zr
3.2. Ordination analyses of XRF data in ST3c (number of indivduals = 320)
a. Multivariate ordination in ST3c from PAST (matrix correlation)
Pc1 (52%)
Pc2 (20%)
b. Multivariate ordination in ST3c from XELERATE
Biplot with cluster repartition
Cluster 1
Cluster 2
Cluster 3
Cluster 4
Component 1 (expl. var. = 51.8%)
Component 2 (expl. var. = 20.2%)
c. Along core (ST3c) map distribution of the 4 clusters identified with Xelerate
Depth (cm) in core ST3c
Cluster 2 group with: homogeneous with S
Cluster 3 group with: Y, Br, Pb
Cluster 4 group with: Ti, Mn, Fe, Rb
Cluster 1 group with: Ca, Sr, Zr (minor S)

Figure 3

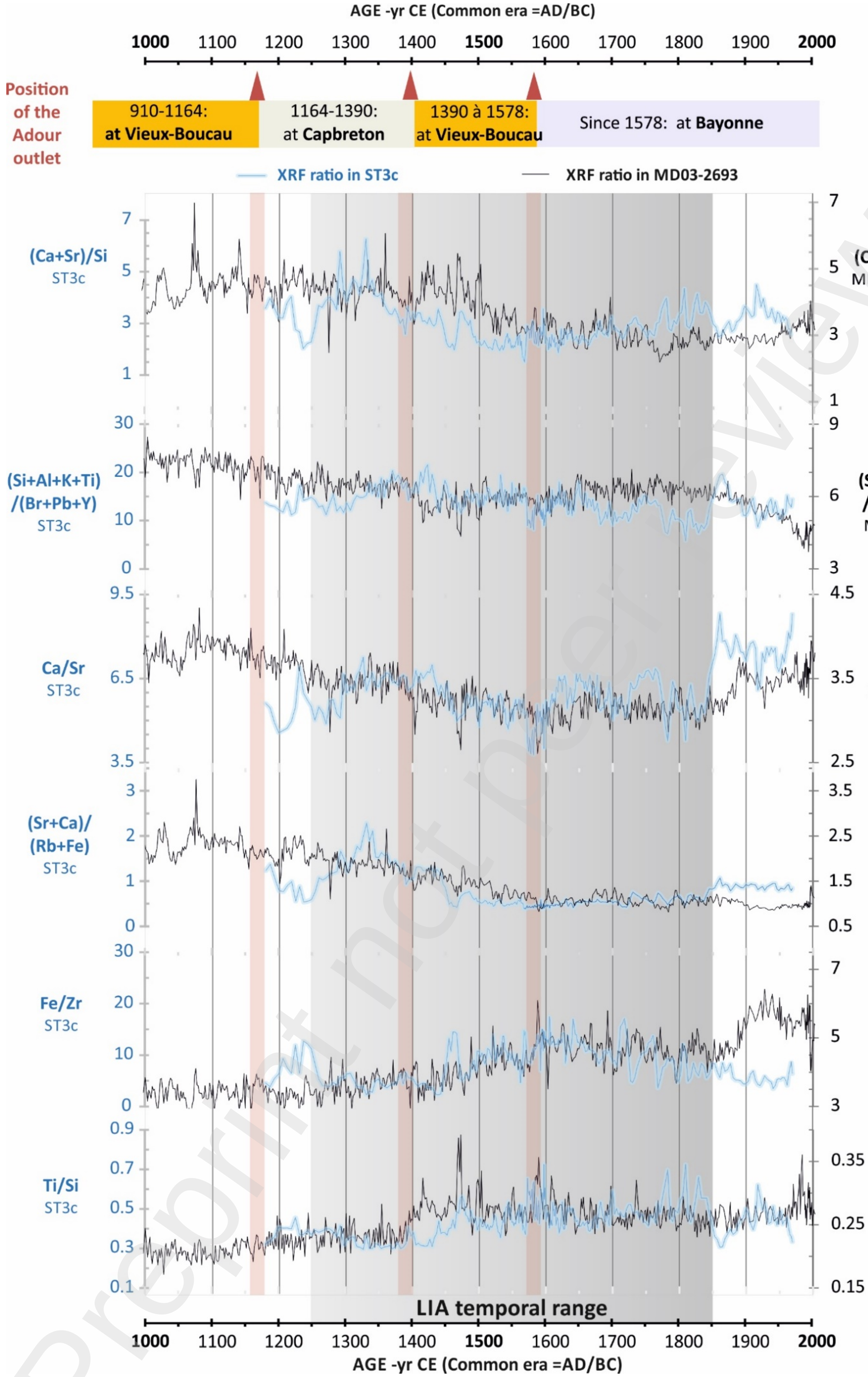

994

995 **Figure 4**

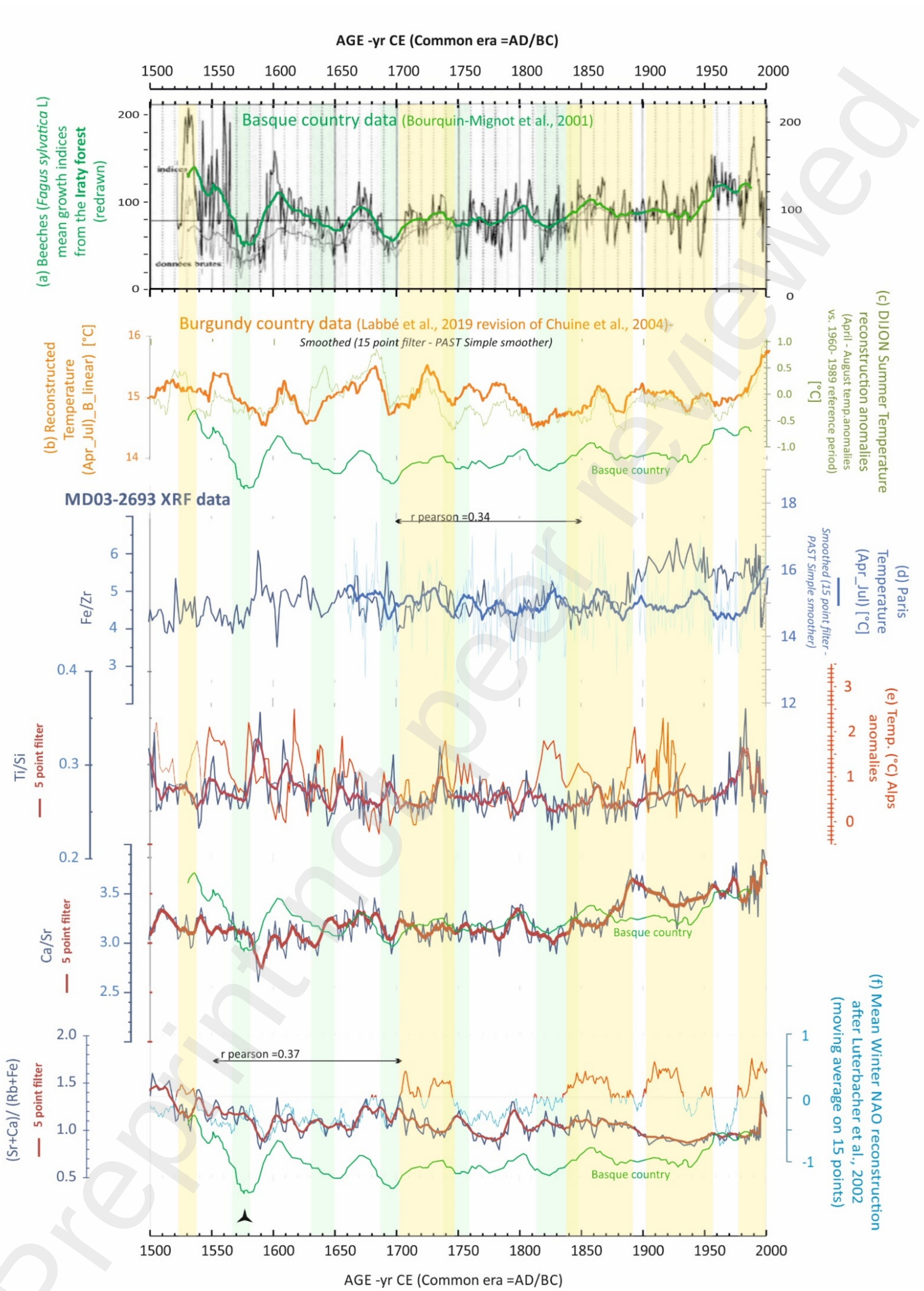
AGE -yr CE (Common era =AD/BC)
1500 1550 1600 1650 1700 1750 1800 1850 1900 1950 2000
(a) Beeches (Fagus sylvatica L) mean growth indices from the Iraty forest (redrawn)
Basque country data (Bourquin-Mignot et al., 2001)
indices
données brutes
200
100
0
Burgundy country data (Labbé et al., 2019 revision of Chuine et al., 2004)
Smoothed (15 point filter - PAST Simple smoother)
(b) Reconstructed Temperature (Apr_Jul)_B_linear) [°C]
16
15
14
(c) DIJON Summer Temperature reconstruction anomalies (April - August temp.anomalies vs. 1960- 1989 reference period) [°C]
1.0
0.5
0.0
-0.5
-1.0
Basque country
MD03-2693 XRF data
r pearson =0.34
Fe/Zr
6
5
4
3
(d) Paris Temperature (Apr_Jul) [°C]
Smoothed (15 point filter - PAST Simple smoother)
18
16
14
12
Ti/Si
5 point filter
0.4
0.3
0.2
(e) Temp. (°C) Alps anomalies
3
2
1
0
Ca/Sr
5 point filter
3.5
3.0
2.5
2.0
Basque country
(Sr+Ca)/ (Rb+Fe)
5 point filter
r pearson =0.37
1.5
1.0
0.5
Basque country
(f) Mean Winter NAO reconstruction after Luterbacher et al., 2002 (moving average on 15 points)
1
0
-1
1500 1550 1600 1650 1700 1750 1800 1850 1900 1950 2000
AGE -yr CE (Common era =AD/BC)

Figure 5

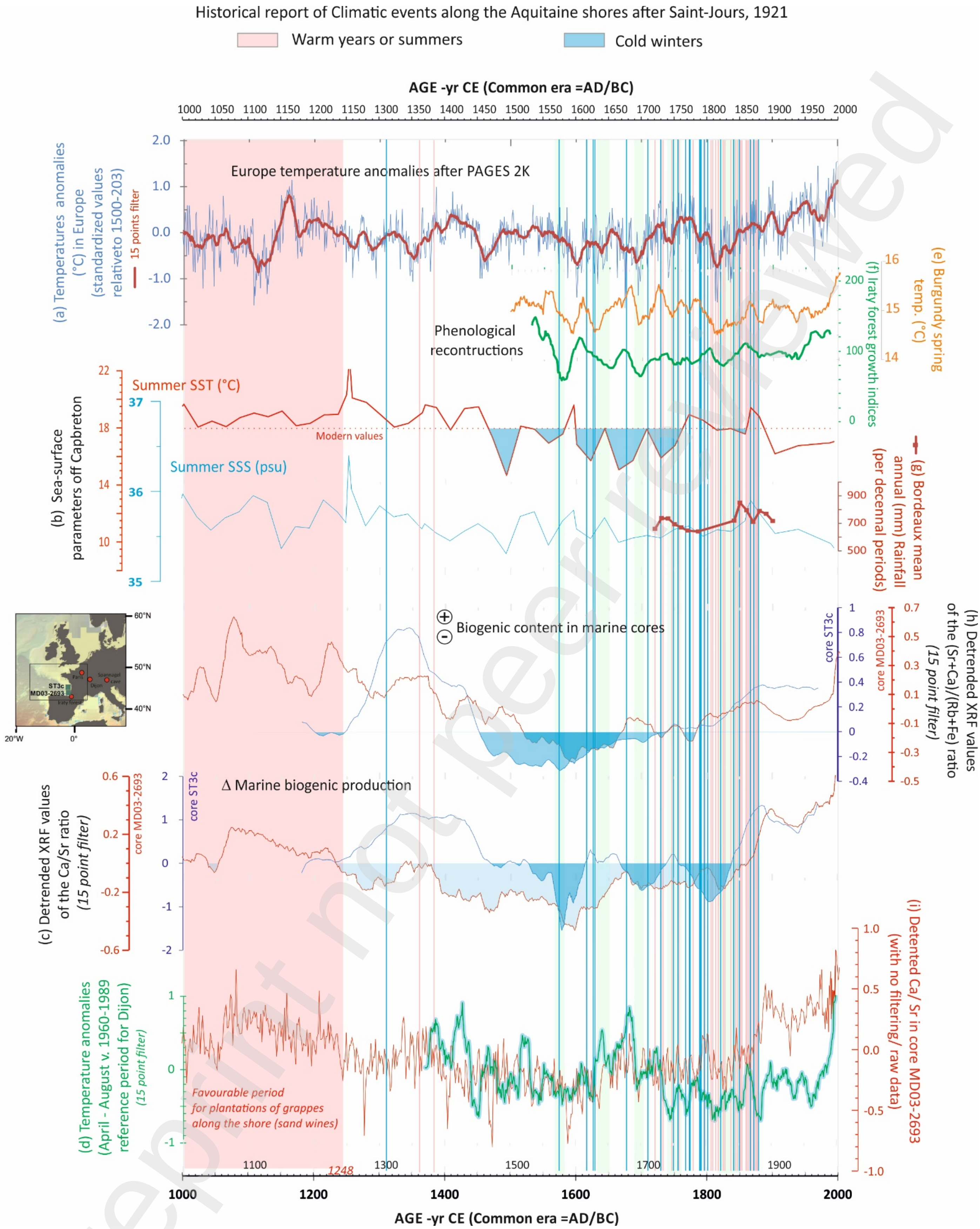

998

999 **Figure 6**

Table caption

Table 1: information and references concerning the studied cores.

Table 2: detailed list of dating results. For radiocarbon ages, raw data are given together with the calibrated results (mean for the 1 sigma range) after the new Calib8.1.0 curves. Both cal-BP and AD/BC (CE) results are provided but figures have been built in year CE.

Table 3: Pearson correlation coefficients in between some key series (see Figure 5). The calculations have been done with Excel (Data Analysis ToolPak) and also verified with the PAST4.09 software (Hammer et al., 2001, using the *Correlation* tool in the *Univariate* menu) after a sampling of data every 2 years also done with PAST (with the *Regular interpolation* tool -linear method- in the *Transform* menu).

Core label	*Cruise references, DOI*	*Latitude °N*	*Longitude ° E*	*Water depth (m)*	*Longitudinal distance (km) from the shore*	*References, Datasources*
MD03-2693	SEDICAR/PICABIA, SEDICAR MD 133, RV Marion Dufresne, BOURILLET Jean-François, TURON Jean-Louis (2003) https://doi.org/10.13155/36807	43.6543	-1.6634	431	15	**This work,** Gaudin et al., 2006, Mary et al., 2015, 2017
JB7-ST3c	JERICOBENT-7 cruise, RV Côtes De La Manche, DEFLANDRE Bruno (2019) https://doi.org/10.17600/18001022	45.6822	-1.6932	58	50	**This work**

Table 1

Core label	Mid-depth of the sampled interval in the core (cm) - uncrorrected from coring artefacts	Dated material	Labcode	Age Raw ^{14}C (a BP /error)	*Calibrated age (a BP) -Mean value - Calib8.1 Mean 1 sigma Cal BP (-400 / Intcal20)*	Calib8.1 One Sigma Ranges: cal BP [start:end] relative area	Calib8.1 Two Sigma Ranges: cal BP [start:end] relative area	*Calib Ref. delta R, curve ref.*	***Calendar Age yr BP (used for the revised age model)***	**Calendar Age (yr AD)**	*For comparison : Calendar Age yr AD (Calib 5.1.0. for radiocarbon datings) Mary et al 2015, 2017*
MD03-2693	1	Bulk sediment, 210Pb et 137 Cs	EPOC Cs/Pb	*Not relevant (Radionucleides)*					***-53,0***	**2003**	*2003*
MD03-2693	6	Bulk sediment, 210Pb et 137 Cs	EPOC Cs/Pb						***-51,0***	**2001**	*2001*
MD03-2693	11	Bulk sediment, 210Pb et 137 Cs	EPOC Cs/Pb						***-46,9***	**1997**	*1997*
MD03-2693	21	Bulk sediment, 210Pb et 137 Cs	EPOC Cs/Pb						***-45,6***	**1996**	*1996*
MD03-2693	61	Bulk sediment, 210Pb et 137 Cs	EPOC Cs/Pb						***-37,0***	**1987**	*1987*
MD03-2693	72,5	Bulk sediment, 210Pb et 137 Cs	EPOC Cs/Pb						***-29,0***	**1979**	*1979*
MD03-2693	122,5	Bulk sediment, 210Pb et 137 Cs	EPOC Cs/Pb						***3,0***	**1947**	*1947*
MD03-2693	157,5	Bulk sediment, 210Pb et 137 Cs	EPOC Cs/Pb						***53,0***	**1897**	*1897*
MD03-2693	1193	Mollusc Shell Gaudin et al	Poz-9338	1445±30	941,5	[924: 959] 1,	[914: 998] 0,912262	*Marine sample using Delta R = 400±3, Calibration data set: intcal20.14c, # Reimer et al. 2020*	***941,5***	**1008,5**	*960*
MD03-2693	2184	Mollusc Shell Gaudin et al	Poz-9339	2305±30	1806,5	[1779: 1834] 0,638495	[1732: 1890] 0,985993		***1806,5***	**143,5**	*34*
MD03-2693	2288	Mollusc Shell Gaudin et al	Poz-9340	2390±30	1916	[1886: 1946] 0,736331	[1866: 1994] 0,925822		***1916***	**34**	*-75.5*
JB7 -ST3c	1,5	Bulk sediment, 210Pb et 137 Cs	EPOC Cs/Pb	*Not relevant (Radionucleides)*					***-18,4***	**1968**	
JB7 -ST3c	11,5	Bulk sediment, 210Pb et 137 Cs	EPOC Cs/Pb						***8,9***	**1941**	
JB7 -ST3c	25,5	Bulk sediment, 210Pb et 137 Cs	EPOC Cs/Pb						***47,2***	**1903**	
JB7 -ST3c	89,5	Mollusc bivalve shell, *Acanthocardia tuberculata* ?	SacA62020	615±30	288,5	[276: 301] 0.358239	[143: 220] 0.533656	*Marine sample using Delta R = 400±3, Calibration data set: intcal20.14c, # Reimer et al. 2020*	**288,5**	**1662**	
JB7 -ST3c	108,5	Mollusc gastropod shell, *Actalon sp.?*	SacA60911	640±35	296	[278: 314] 0.580247	[264: 321] 0.459406		**296,0**	**1654**	
JB7 -ST3c	149,5	Mollusc gastropod shell (completed by small skeletons of juvenile benthics)	SacA68043	<u>685±30</u>	<u>407,5</u>	[389: 426] 0.549808	[351: 448] 0.62673		**<u>Discarded</u>**		
JB7 -ST3c	199,5	Mollusc bivalve shell fragments, *Abra sp.*	SacA68044	725±30	385	[357: 413] 0.59703	[309: 467] 1.		**385,0**	**1565**	
JB7 -ST3c	249,5	Mollusc shell fragments	SacA68045	765±30	456,5	[430: 483] 0.579724	[422: 496] 0.512975		**456,5**	**1494**	
JB7 -ST3c	269,5	Benthic foramnifera : *Ammonia tepida + Quinqueloculina laevigata*	SacA68049	<u>1545±30</u>	<u>1005</u>	[975: 1035] 0.694122	[960: 1082] 0.812252		**<u>Discarded</u>**		
JB7 -ST3c	269,5	Mollusc bivalve shells (completed by small skeletons of juvenile benthics)	SacA68050	875±30	515	[504: 526] 1.	[494: 541] 1.		**515,0**	**1435**	
JB7 -ST3c	298,5	Mollusc gastropod shells, juvenile *Turritella* sp.	SacA60912	1080±35	658	[646: 670] 0.624572	[627: 677] 0.600845		**658,0**	**1292**	
JB7 -ST3c	302,5	Mollusc gastropod shells, juvenile *Turritella* sp.	SacA60913	1025±30	636,5	[624: 649] 0.444304	[552: 654] 1.		**636,5**	**1314**	

1015

Table 2

Time period	Tested on the whole period covered in common by the series			Tested on the specific intervals of common coverage					
	Between 1080 and 1934 CE	Between 1500 and 2000 CE	Between 1660 and 2002 CE	Between 1080 and 1850 CE	Between 1500 and 1934 CE	Between 1650 and 1850	Between 1600 and 1800 CE	Between 1550 and 1700 CE	Between 1700 and 1850 CE
Tested parameters	**Temp [°C] Alps** *(data resampled every 2 years)*	**NAO winter index** *(smothed with a 15 point filter and resampled every 2 years)*	**Paris_Temperature (Apr_Jul) [°C]** *(smothed with a 15 point filter and resampled every 2 years)*	***Temp [°C] Alps*** *(data resampled every 2 years)*			**NAO winter index** *(smothed with a 15 point filter and resampled every 2 years)*		**Paris_Temperature (Apr_Jul) [°C]** *(smothed with a 15 point filter and resampled every 2 years)*
Fe/Zr 2693 (data resampled every 2 years)	-0.386	0.215	0.005	Correlation not tested	Correlation not tested	Correlation not tested	Correlation not tested	Correlation not tested	0.341
Ti/Si 2693 (data resampled every 2 years)	-0.528	-0.078	Correlation not tested	-0.544	0.087	0.047	Correlation not tested	Correlation not tested	Correlation not tested
Ca/Sr 2693 (data resampled every 2 years)	0.539	0.326	Correlation not tested	0.549	0.063	-0.192	Correlation not tested	Correlation not tested	Correlation not tested
(Sr+Ca)/(Rb+Fe) 2693 (data resampled every 2 years)	0.572	*-0.045*	Correlation not tested	0.599	Correlation not tested	Correlation not tested	0.274	0.374	Correlation not tested
	(yellow)	significative values		xxx improved values of correlation					

Table3